EFFECTS OF SHADING ON THE POWER DELIVERY OF SOLAR PANELS

BY

AZAKA KENNETH AZAKA	**ENG2002217**
AZEKE OSEREMHEN BENNETT	**ENG2002218**
BENEDICT OSAMUDIAMEN	**ENG2002219**
BERAMO BENJAMIN IYUATER	**ENG2002220**
CHIEKWE EKENEM	**ENG2002221**
UKADIKE COLLINS	**ENG2002222**
DOGHOR MICHEAL OGHENEOVIE	**ENG2002223**
EREMWANARUE OSAKPOLOR DESTINY	**ENG2002237**
IMONJE GODSWILL OSEIWE	**ENG2002257**
DIVINE FAVOUR OMORUYI	**ENG2002306**
JAMGBADI OSEADALE MOSES	**ENG2006265**

A PROJECT SUBMITTED TO

THE DEPARTMENT OF ELECTRICAL AND ELECTRONICS ENGINEERING, FACULTY OF ENGINEERING.

UNIVERSITY OF BENIN, BENIN CITY.

OCTOBER 2025

CERTIFICATION

This is to certify that the research work titled “Effects of Shading on the Power Delivery of Solar Panels” was carried out by AZAKA KENNETH AZAKA, AZEKE OSEREMHEN BENNETT, BENEDICT OSAMUDIAMEN, BENJAMIN IYUATER BERAMO, CHIEKWE EKENEM, UKADIKE COLLINS, DOGHOR MICHEAL OGHENEOVIE, EREMWANARUE OSAKPOLOR DESTINY, IMONJE GODSWILL OSEIWE, DIVINE FAVOUR OMORUYI, JAMGBADI OSEADALE MOSES, with matriculation number: ENG2002217, ENG2002218, ENG2002219, ENG2002220, ENG2002221, ENG2002222, ENG2002223, ENG2002237, ENG2002257, ENG2002306, ENG2006265 in total fulfilment of the requirements for the award of Bachelor of Engineering in University of Benin.

_____ _____

Engr. Dr. Omorogiuwa O. S. Date

(Project Supervisor)

_____ _____

Engr. Dr. Omorogiuwa O. S Date

(Head of Derpartment)

DEDICATION

We dedicate this work to God, whose unwavering support, encouragement and guidance have been invaluable throughout this journey.

ACKNOWLEDGMENTS

To God: Your divine grace and unwavering presence in our lives have been a constant source of strength and inspiration. We are profoundly thankful for the blessings, wisdom, and inner strength that you have provided, guiding us through the journey.

We extend our heartfelt gratitude to Engr. Dr. Omorogiuwa O. S for his invaluable guidance and support throughout this research. Our sincere appreciation goes to the University of Benin for providing the necessary resources.

To the Head of Department (HOD), Engr. Dr. Omorogiuwa O. S: Your leadership, encouragement, and commitment to academic excellence have been instrumental in shaping our academic and research paths. Your guidance and support have helped us navigate the challenges and complexities of this project.

Special thanks to our families, our friends and colleagues for their encouragement and unwavering support.

ABSTRACT

Solar photovoltaic (PV) technology is a critical low-carbon solution, but its performance is severely compromised by shading. This study addresses the persistent problem of partial shading, which causes disproportionate power losses and creates thermal stress risks like hot spots.This research aims to quantify the effect of shading on PV panel voltage, current, and power output under controlled laboratory conditions.The methodology employed an experimental approach using an SES TPS-3720 Solar Energy Trainer. Experiments measured performance under 0% (baseline), 50% (partial), and 100% (full) shading.The study also evaluated the impact of shading material optical properties by testing opaque (wood), semi-opaque (paper), and translucent (plastic film) materials. Measurements were recorded across five irradiance levels using both LED lamp and DC motor loads.Key findings demonstrate a highly non-linear performance degradation. Partial shading covering 50% of the panel area resulted in a 65-70% power loss, far exceeding a proportional reduction.Full shading with opaque (wood) or semi-opaque (paper) materials caused a 100% power loss, eliminating all usable current. Translucent plastic film caused the least degradation (approx. 23% power loss).The results confirm that a material's optical transmittance, not its physical density, is the dominant factor determining shading severity.These findings validate established photovoltaic theory and highlight the critical importance of shadow avoidance in system design. The study reinforces the necessity of mitigation strategies such as bypass diodes and module-level power electronics (MLPE) in shade-prone installations.

LIST OF ABBREVIATIONS

Abbreviation	Full Form
AC	Alternating Current
AM	Air Mass
ANN	Artificial Neural Network
API	Application Programming Interface
BL	Bridge-Linked
DC	Direct Current
DSSC	Dye-Sensitised Solar Cell
FF	Fill Factor
GW	Gigawatt
HC	Honey-Comb
I-V	Current-Voltage
I_mp	Current at Maximum Power Point
I_sc	Short-Circuit Current
IEC	International Electrotechnical Commission
IRENA	International Renewable Energy Agency
LCD	Liquid Crystal Display

LDPE	Low-Density Polyethylene
LED	Light-Emitting Diode
mA	Milliampere (10^{-3} ampere)
MLPE	Module-Level Power Electronics
MPP	Maximum Power Point
MPPT	Maximum Power Point Tracking
mW	Milliwatt (10^{-3} watt)
P&O	Perturb and Observe
P-V	Power-Voltage
PET	Polyethylene Terephthalate
PSO	Particle Swarm Optimisation
PV	Photovoltaic
PVC	Polyvinyl Chloride
SAM	System Advisor Model
SES	Scientific Educational Systems
SI	International System of Units (Système International)
STC	Standard Test Conditions
TCT	Total Cross-Tied

TPS	Training Panel System
UV	Ultraviolet
V	Volt
V_mp	Voltage at Maximum Power Point
V_oc	Open-Circuit Voltage
W	Watt
W/m²	Watts per Square Meter

TABLE OF CONTENTS

CHAPTER ONE

INTRODUCTION

1.1 Background to the Study

The world's appetite for energy continues growing, and as climate concerns intensify, the push toward sustainable, low-carbon solutions has never been stronger. Among renewable energy sources, solar photovoltaic (PV) technology stands out because it converts sunlight directly into electricity—no moving parts, no emissions during operation, just clean power from an abundant natural resource. This simplicity and environmental appeal have driven rapid adoption worldwide, particularly in regions blessed with high solar irradiance. Yet for all its promise, PV technology faces a persistent challenge: its performance depends entirely on uniform sunlight reaching the panel surface (Mehedi et al., 2021).

Enter shading—perhaps the most underestimated obstacle to solar efficiency. Trees swaying in the wind, utility poles casting long shadows, neighbouring buildings blocking morning sun, even the panel array's own mounting structure can obstruct light and dramatically reduce output. Shading takes various forms: sometimes the entire module sits in shadow, but more commonly only certain cells are affected while others receive full illumination. This partial shading proves particularly troublesome due to how PV modules are electrically configured. Most modules connect their cells in series to achieve practical voltage levels, but this arrangement creates a vulnerability. When one or more cells receive less sunlight than their neighbours, they limit current flow through the entire string—like a kinked garden hose restricting water flow regardless

of pressure upstream. The result? Power losses often far exceed what the shaded area alone would suggest (Fetanat et al., 2022; Siddiqui et al., 2024).

Recent investigations have revealed the severity of this mismatch effect. Studies document cases where shading a single cell—perhaps just 2-3% of total panel area—reduces overall output by 30% or more. These losses don't scale linearly; small shaded regions can trigger disproportionately large performance drops because they force the entire series string to operate at reduced current. Even more problematic, partial shading creates multiple peaks in the power-voltage curve, confusing maximum power point tracking (MPPT) systems that assume a single, well-defined maximum. Without sophisticated global MPPT algorithms or module-level power electronics that allow each panel to operate independently, systems often settle into suboptimal operating points, extracting far less energy than conditions would otherwise permit (Mehedi et al., 2021; Siddiqui et al., 2024).

Beyond immediate power reduction, shading introduces thermal stress that threatens long-term module integrity. When brighter cells force current through shaded neighbours, those shaded cells can't generate enough voltage to pass that current comfortably—they operate in what's called reverse bias, dissipating energy as heat rather than contributing to the circuit's output. This creates localised hot spots that can reach temperatures high enough to degrade encapsulation materials, crack semiconductor wafers, or, in extreme case,s pose fire hazards. Thermal imaging studies combined with electrical performance measurements reveal that hotspot severity doesn't always correlate simply with shading percentage, suggesting complex interactions between thermal and electrical phenomena that warrant careful investigation (EPJ Photovoltaics, 2024; Energies, 2024).

The solar industry hasn't ignored these challenges. Modern PV modules incorporate bypass diodes—semiconductor devices that provide alternate current paths around shaded cell groups, reducing voltage drops and preventing the most severe thermal stress. More advanced installations employ module-level power electronics such as microinverters or DC power optimisers that perform MPPT at the individual panel level, effectively isolating each module's performance from its neighbours. Alternative array wiring configurations like total-cross-tied or bridge-linked arrangements distribute current more evenly when shading occurs, limiting the impact of any single obstructed cell. These mitigation strategies work, but they add cost and complexity. Strategic site selection and careful shading analysis during system design often prove more economical than solving problems with expensive hardware after installation (Siddiqui et al., 2024; Mehedi et al., 2021; IEA-PVPS, 2024).

In practice, completely avoiding shading proves difficult, particularly in environments where solar installations proliferate. Urban rooftops contend with neighbouring buildings and street trees. Rural installations face vegetation that grows taller each year, gradually encroaching on what were once shadow-free panels. Even carefully planned ground-mounted arrays experience row-to-row shading during early morning and late afternoon when the sun hangs low on the horizon. Over a 25-year installation lifespan, conditions change—trees mature, new construction rises nearby, and accumulated soiling creates localised shadows that weren't present during commissioning. Understanding how these shadows affect PV output—both instantaneously and cumulatively over time—becomes essential for accurate performance prediction, realistic economic analysis, and safe long-term operation (Fetanat et al., 2022).

Despite significant advances in understanding and mitigating shading effects, gaps remain in the research landscape. Much existing work focuses on large commercial arrays or individual cells tested in isolation, with less attention paid to the educational solar trainers used in technical training programs worldwide. These trainers occupy a middle ground—more complex than single-cell setups but simpler than utility-scale installations—making them valuable both as teaching tools and as experimental platforms. Real-world data from developing nations, where rooftop installations often face challenging shading conditions from dense urban environments or abundant vegetation, remains scarce. Many simulation models still struggle to accurately capture the complexity of partial shading, particularly when dynamic elements like passing clouds, bird shadows, or wind-blown tree branches create rapidly changing irradiance patterns.

This study aims to address these gaps through a systematic investigation of how various shading types and intensities affect solar panel performance. By combining controlled laboratory experiments with careful measurement of voltage, current, and power under realistic shading scenarios, the research provides quantitative data applicable both to educational contexts and practical system design decisions.

1.2 Statement of the Problem

Solar photovoltaic systems have become a cornerstone of the global transition to clean electricity, with installations spanning residential rooftops, commercial buildings, and utility-scale solar farms. Yet for all their environmental benefits and increasingly competitive economics, PV systems face a persistent performance challenge that continues to frustrate installers, system designers, and owners alike: partial shading.

When objects like buildings, poles, trees, or even the system's own mounting hardware block sunlight from reaching portions of a panel, the resulting power loss often far exceeds what simple proportional calculations would predict. A tree branch casting a shadow over 20% of a panel's surface might reduce output by 50% or more—a disproportionate impact that stems from the series electrical connections within the module. Studies document cases where even a single shaded cell dramatically reduces the current flow through an entire string of series-connected cells, effectively throttling the whole panel's output to match the weakest link (Özkalay et al., 2024).

The problem extends beyond simple power reduction. Shaded cells forced to conduct current from brighter neighbours can develop dangerous hot spots—localised regions of excessive heating that accelerate material degradation and, in severe cases, pose safety hazards. These thermal stresses compound over time, potentially shortening module lifespan and increasing the likelihood of premature failure. What makes this particularly concerning is that hot spot formation doesn't always correlate obviously with the amount of shading; electrical mismatch patterns and thermal dissipation characteristics interact in complex ways that simple visual inspection can't predict.

Partial shading also complicates the electrical behaviour that inverters and charge controllers must manage. Under uniform illumination, a PV module's power-voltage curve exhibits a single, clearly defined peak where power output reaches maximum. Shading disrupts this simplicity, creating multiple local maxima that confuse conventional maximum power point tracking algorithms. The system might settle on a local peak rather than the true global maximum, extracting perhaps 60-70% of available power when better tracking could recover 90% or more. The shape and pattern of shading matter too—rectangular shadows affect performance differently than triangular

ones, and the orientation of shadow edges relative to cell layout influences how severely output drops (EEWorldOnline, 2025; Alnakhlani & Selimli, 2025).

Current international testing standards, including IEC 61215-2:2021, address shading effects to some degree, but they may not fully capture the conditions that real-world installations experience. Laboratory tests typically employ uniform opaque masks to create well-defined shaded regions, while actual installations contend with translucent clouds, dust accumulation that gradually reduces light transmission, and dynamic shadows from swaying branches or passing birds. Urban environments in developing countries present particularly challenging conditions—dense construction, narrow streets creating morning and evening shadows, vegetation growth that accelerates in tropical climates—yet research focusing on these contexts remains limited.

This study responds to that need by systematically examining how different shading conditions affect power delivery in photovoltaic panels, using controlled experiments that bridge the gap between idealised laboratory conditions and the messy reality of operational installations.

1.3 Significance of the Study

This research makes several distinct contributions to photovoltaic science and engineering practice, addressing gaps in current understanding while providing immediately applicable insights for system design and installation.

Educational Value and Institutional Context:

Most shading research concentrates on commercial installations where stakes are measured in megawatts and millions of dollars. While understandable given the scale of investment involved, this focus has left educational solar trainers largely unstudied

despite their widespread use in technical programs worldwide. These trainers—systems like the SES TPS-3720 used in this study—serve thousands of engineering students annually, yet their specific response to shading remains poorly documented. Understanding how they behave under various shadow conditions enhances their pedagogical value while providing experimental validation that can scale to larger systems. The data generated here directly supports curriculum development and laboratory exercise design at institutions teaching renewable energy technology.

Material Characterisation Across Optical Properties:

Previous shading studies typically employ binary conditions: cells are either fully illuminated or completely blocked by opaque masks. Real-world obstructions rarely exhibit such extremes. Clouds transmit diffuse light even while blocking direct sunlight. Dust accumulation gradually dims panels rather than creating sharp shadow boundaries. Tree canopies filter sunlight through layers of leaves with varying density. This research examines three materials representing the full spectrum of optical behaviour—opaque wood (complete blockage), semi-opaque paper (minimal transmission), and translucent plastic film (substantial transmission). By quantifying performance across this gradient, the study reveals how gradual reductions in light availability affect output, information directly applicable to predicting real installation behaviour under diverse atmospheric and environmental conditions.

Load-Dependent Response Investigation:

Solar panels power remarkably diverse loads: resistive heating elements, inductive motors, capacitive power supplies, battery charging systems, and grid-tied inverters all present different electrical characteristics to the PV source. Yet most research measures panel performance into idealised resistive loads that don't reflect this variety. This study

compares two fundamentally different load types—a resistive LED lamp and an inductive DC motor—revealing how electrical characteristics influence shading response. The motor's lower resistance and higher current draw versus the lamp's higher impedance and lower current create different operating points on the I-V curve, potentially affecting which parts of the curve become accessible under partial shading. These findings inform system matching decisions: should a particular application use motors or lamps, given expected shading patterns? How does load selection interact with panel selection and array configuration?

Methodological Accessibility and Replication:

Much published research employs specialised equipment, custom measurement systems, or commercial testing facilities that limit who can replicate or extend the work. Educational institutions in developing regions often lack such resources despite having motivated students and faculty interested in renewable energy. This study deliberately uses an educational trainer system and standard laboratory instruments available at most engineering departments. By documenting procedures in detail—including seemingly mundane details like stabilisation times, connection sequences, and troubleshooting approaches—the methodology becomes accessible to other institutions. The MATLAB code provided in the appendices enables direct replication of analysis techniques. This democratisation of experimental approach supports the growth of distributed research capacity, allowing institutions worldwide to contribute to expanding the knowledge base.

Quantitative Design Guidelines:

Beyond contributing to scientific understanding, this research generates practical guidance for installation professionals and system designers. How much shading is

acceptable before performance becomes unacceptable? What power loss should designers expect from partial versus complete obstruction? Does shading material matter, or only the percentage of light blocked? The experimental data answers these questions with specific numbers: 50% panel coverage reduces power by approximately 65-70% for typical loads, far exceeding proportional expectations. Translucent materials like thin plastic cause modest degradation (around 23% power loss) while opaque obstructions create near-total failure. These concrete figures support go/no-go decisions during site assessment: Is that tree shadowing the proposed installation acceptable, or should panels be relocated? Will accumulated dust require monthly cleaning or quarterly cleaning? How much output degradation justifies investing in expensive module-level power electronics?

These contributions build upon substantial prior research that established a foundational understanding of shading phenomena. Duranay and Güldemir (2025) demonstrated through simulation and experiment that environmental shading from buildings, trees, and dust accumulation could reduce output by 50% or more, with bypass diodes providing meaningful mitigation. Wilson et al. (2020) documented how shading alters I-V characteristics and complicates MPPT, particularly when mismatch losses create multiple power peaks. Bonnassieux et al. (2021) developed shading ratio metrics and image-based modelling techniques for predicting performance under shadow conditions, validating these tools against field measurements. Jost et al. (2022) explored alternative cell geometries—radial and spiral layouts that distribute current more evenly—as design solutions for reducing shading sensitivity. This study extends these efforts by providing systematic experimental validation under controlled conditions, using equipment and methods accessible to a broad research community, and examining material and load variations often overlooked in previous work. The results bridge the

gap between theoretical understanding documented in literature and practical knowledge needed for day-to-day installation and design decisions (Guiliano et al., 2021).

1.4 Aims and Objectives

This study aims to quantify the effect of shading on the voltage, current, and power output of photovoltaic panels under controlled laboratory conditions.

The specific objectives are:

1. To establish baseline electrical performance characteristics (voltage, current, and power output) of the solar panel under unshaded conditions across varying irradiance levels, providing reference values for subsequent comparison.
2. To quantify performance degradation under partial shading (50% panel coverage) and full shading (100% coverage) conditions, determine the relationship between shaded area and power loss.
3. To evaluate the impact of shading material optical properties by testing opaque (wood), semi-opaque (paper), and translucent (plastic film) materials under full panel coverage, isolating the effect of light transmission characteristics on electrical output.

4. To analyse the combined effects of irradiance level and shading severity, establish quantitative performance metrics across the full range of tested conditions for application to system design and performance prediction.

1.5 Methodology

This study employs an experimental approach using the SES TPS-3720 Solar Energy Trainer to investigate shading effects on photovoltaic performance. The methodology consists of:

1. **Baseline Measurements:** The voltage and current of the PV panel will be measured under uniform light intensity at five irradiance levels (20%, 40%, 60%, 80%, 100% lamp power) with no shading applied, using both LED lamp and DC motor loads to establish reference performance values.

2. **Shading Coverage Analysis:** The panel will be subjected to partial shading (50% coverage) and full shading (100% coverage) using paper as the shading material, with voltage and current measurements recorded at all irradiance levels for both load types to quantify coverage-dependent power losses.

3. **Material Density Evaluation:** The panel will be fully shaded using three different materials—opaque wood, semi-opaque paper, and translucent plastic film—to evaluate how material optical properties affect power output under identical light intensity conditions.

4. **Data Analysis:** All experimental data will be processed using MATLAB R2024b to compute instantaneous power, mean power, and percentage performance reductions, with results presented through power-versus-irradiance curves and comparative bar charts.

1.6 Scope of the Study

This research focuses specifically on quantifying shading effects under controlled laboratory conditions using a single educational solar trainer panel. The scope encompasses:

Included Elements:

- Static shading scenarios with fixed shadow positions
- Three distinct material types representing a spectrum of optical properties
- Two load types with different electrical characteristics
- Five irradiance levels spanning low to high light intensity
- Voltage, current, and power measurements as primary performance indicators
- Single-panel configuration without array-level interactions

Excluded Elements:

- Outdoor field testing under natural sunlight and weather variations
- Dynamic shading from moving clouds or wind-blown obstacles
- Long-term degradation effects over months or years
- Temperature variation studies and thermal stress analysis
- Multi-panel array configurations and string-level mismatch effects
- Advanced mitigation technologies (microinverters, power optimisers, MPPT algorithms)
- Economic analysis and return-on-investment calculations

These boundaries enable focused investigation of fundamental shading mechanisms while acknowledging that practical installations involve additional complexities beyond the study's scope.

1.7 Organisation of the Thesis

- **Chapter One:** Introduction, problem statement, objectives, and methodology
- **Chapter Two:** Literature review on photovoltaic systems, shading effects, and mitigation strategies
- **Chapter Three:** Detailed experimental methodology, equipment specifications, and measurement procedures
- **Chapter Four:** Results presentation, data analysis, graphical visualisations, and interpretation
- **Chapter Five:** Conclusions, recommendations, limitations, and suggestions for future research

CHAPTER TWO

LITERATURE REVIEW

This chapter examines the existing body of research on photovoltaic systems with particular emphasis on how shading affects their performance. The review begins with fundamental principles of solar energy conversion, then progressively narrows its focus to shading phenomena—exploring different types, their measurable impacts, and the various mitigation strategies that have emerged from decades of research. Understanding these prior contributions provides the necessary context for appreciating both the significance of this study and the gaps it aims to address.

2.1 Overview of Solar Energy Systems

Over the past two decades, solar photovoltaic technology has transformed from a niche renewable energy solution into a mainstream power generation option. This shift has been driven by converging factors: growing awareness of climate change, declining manufacturing costs, and steady improvements in conversion efficiency. By 2023, global installed PV capacity reached approximately 1,954.6 gigawatts, representing roughly 40% of total renewable energy capacity worldwide (IRENA, 2024). What makes these numbers particularly striking is the speed at which they've been achieved—solar installations are projected to meet 45% of global energy demand by 2050, according to forecasts by Herez et al. (2016).

The appeal of photovoltaic systems extends beyond their environmental credentials. Unlike conventional power plants, PV installations operate silently, require minimal maintenance once installed, and can be deployed at scales ranging from small residential rooftops to sprawling utility-grade solar farms (Twidell & Weir, 2015; Kalogirou, 2009). Their modular

nature allows for flexible design configurations, while their solid-state operation—with no moving parts—contributes to operational lifespans often exceeding 25 years. Recent years have seen manufacturing costs decline steadily, making solar energy increasingly competitive with fossil fuel alternatives even without subsidies (IRENA, 2020).

Research attention has naturally concentrated on maximising system performance. Xuesong Zhou et al. (2018) and Haque & Zaheeruddin (2013) identified several critical areas: optimising module characteristics, developing more efficient power conversion electronics, refining maximum power point tracking algorithms, and ensuring system stability under varying conditions. Malinowski et al. (2017) emphasised that both standalone and grid-connected configurations present unique engineering challenges, particularly regarding power quality and integration with existing electrical infrastructure.

At the heart of any photovoltaic system lies the solar cell itself—typically constructed from crystalline silicon, though alternative technologies like dye-sensitised solar cells have emerged as promising alternatives for specific applications (Karthick et al., 2019). The photovoltaic effect, first observed by Edmond Becquerel in 1839 but not practically harnessed until the mid-20th century, remains the fundamental mechanism by which these devices convert sunlight into electrical energy (Ahmad et al., 2014; Müller, 2017). Current commercial systems achieve conversion efficiencies of 20-40% depending on cell technology and operating conditions, though researchers continue pushing toward higher efficiencies through novel materials and cell architectures (Darwish et al., 2022).

Yet even the most advanced photovoltaic technology faces a persistent challenge: environmental factors that compromise performance. Temperature fluctuations, humidity variations, dust accumulation, and—perhaps most significantly—shading can substantially reduce power output (Das, 2019; Rezvani et al., 2022). Chaturvedi & Sharma (2015) observed that partial shading from sources as varied as tree branches, adjacent panels, or bird droppings

can disproportionately affect system performance, often reducing output far more than the percentage of shaded area would suggest.

2.2 Working Principle of Solar Panels

Understanding how shading affects photovoltaic performance requires first grasping the fundamental physics of solar energy conversion. The process begins when photons—particles of light—strike the surface of a solar cell. These cells consist of semiconductor materials, most commonly silicon, which has been specially treated to create distinct electrical properties.

A typical solar cell features two layers of silicon, each "doped" with different elements to alter its electrical characteristics. One layer receives phosphorus atoms, creating an n-type semiconductor with excess electrons. The adjacent layer is doped with boron, producing a p-type semiconductor with a deficit of electrons (or equivalently, an excess of "holes"—the absence of electrons). Where these two layers meet, an electric field naturally forms at what's called the p-n junction. This electric field is crucial—it's what gives the cell its ability to generate electricity.

When sunlight strikes the cell, photons transfer their energy to electrons in the silicon atoms. If a photon carries sufficient energy, it can knock an electron completely free from its atomic bond, creating what physicists call an electron-hole pair. Without the electric field, these electrons and holes would simply recombine, releasing their energy as heat rather than electricity. However, the field at the p-n junction separates them before recombination can occur, pushing electrons toward the n-type region and holes toward the p-type region (Green et al., 2015).

This separation creates an electrical imbalance—an accumulation of negative charge (electrons) on one side and positive charge (holes) on the other. When we connect an external circuit between the two sides, electrons flow through that circuit trying to reunite with the holes, generating direct current (DC) electricity in the process (Kalogirou, 2009). For most practical applications, this DC output must be converted to alternating current (AC) using an inverter, since AC is the standard form of electricity in homes and on power grids.

Individual solar cells produce relatively modest voltage and current—typically around 0.5-0.6 volts per cell under standard conditions. Practical power generation requires connecting multiple cells in series to increase voltage and in parallel to increase current. A typical residential solar panel might contain 60 to 72 cells wired together, producing 250-400 watts under optimal conditions. Larger installations combine multiple panels into arrays capable of generating kilowatts or even megawatts of power.

This series-parallel arrangement, while necessary for achieving useful power levels, introduces a vulnerability that becomes particularly relevant when discussing shading effects. In a series string of cells, current must flow through each cell in sequence—meaning the cell producing the least current effectively becomes a bottleneck limiting the entire string's output. We'll explore the implications of this arrangement more deeply in subsequent sections.

2.3 Shading in Photovoltaic Systems

Shading represents one of the most significant performance challenges facing photovoltaic installations, yet it's often underestimated during system design and site assessment. At its most basic level, shading occurs whenever something blocks sunlight from reaching part or all of a solar panel surface. The obstructions might be permanent fixtures like buildings or utility poles, seasonal variations like deciduous trees that shade panels differently in summer versus winter, or transient phenomena like passing clouds or accumulated snow.

What makes shading particularly problematic is the disproportionate nature of its impact. Intuition might suggest that shading 20% of a panel would reduce output by roughly 20%, but the reality is far more severe. Chouder & Silvestre (2010) documented cases where shading just 10% of a panel's surface area reduced power output by 50% or more. This non-linear relationship stems from the series connection of cells within panels—a configuration necessary to achieve useful voltage levels but which creates a vulnerability to mismatch conditions.

When cells in a series string receive different amounts of light, they generate different amounts of current. Because current must be equal throughout a series circuit, all cells are forced to operate at the current level of the weakest cell—typically the most heavily shaded one. The better-illuminated cells, capable of producing higher current, are effectively throttled back. Even worse, the shaded cells don't simply stop producing power; they become consumers of power, dissipating energy as heat rather than contributing to the circuit's output (Skoplaki & Palyvos, 2009).

This phenomenon can lead to what researchers call "hot spots"—localised areas where shaded cells heat up significantly as they dissipate energy from the rest of the string. Alonso-García et al. (2006) demonstrated that these hot spots can reach temperatures high enough to damage encapsulation materials, crack solar cells, or even start fires in extreme cases. The severity of hot spot formation depends on several factors: the degree of shading, the duration of exposure, the cell's reverse bias characteristics, and whether protective bypass diodes are present and functioning properly.

The impact of shading varies considerably depending on its nature. Static shading from permanent structures produces predictable, consistent losses that can at least be anticipated during system design. A nearby chimney that casts a morning shadow on specific panels will do so reliably every day, allowing installers to potentially work around the issue through

strategic panel placement. Dynamic shading, conversely, presents more complex challenges. Cloud movements create rapidly fluctuating irradiance conditions, while tree branches swaying in the wind produce intermittent shadows that move across panel surfaces unpredictably.

Hasanuzzaman et al. (2016) conducted systematic studies quantifying shading impacts under various conditions. Their findings revealed that even partial shading affecting just 10-20% of a module's area could reduce power output by up to 50%. Perhaps more surprisingly, they found that the pattern of shading matters nearly as much as the total shaded area. A thin shadow crossing multiple cell strings horizontally might cause less damage than the same area concentrated on cells within a single string—a finding with important implications for how we orient panels relative to common shadow sources.

Geographic location and installation orientation further complicate the picture. Panels in equatorial regions experience more overhead sun throughout the year, potentially reducing shadow lengths from nearby obstacles. Higher latitude installations see more dramatic seasonal variations in sun angle, with winter bringing longer shadows that may reach panels easily cleared during summer months. Even the time of day matters—morning and evening shadows stretch longer than midday shadows from the same obstacle.

2.4 Types of Shading

Understanding the various forms shading can take helps both in predicting its impact and in developing appropriate mitigation strategies. Researchers typically categorise shading into several distinct types, each presenting unique challenges for system performance.

External Shading encompasses obstructions originating outside the solar array itself. These divide naturally into permanent and temporary categories. Permanent external shading comes

from fixed structures—the apartment building next door that casts morning shadows, the mature oak tree planted decades ago, or the utility pole positioned along the property line. What distinguishes permanent shading is its predictability. These shadows appear at the same times each day (accounting for seasonal variation), following paths that can be mapped during site surveys. Despite being predictable, permanent shading often proves difficult to mitigate without expensive remediation like tree removal or panel relocation.

Temporary external shading, conversely, exhibits more dynamic behaviour. Clouds drift across the sky, creating shadows that move with wind patterns and weather systems. Young trees grow taller each year, their expanding canopy gradually encroaching on what were once shadow-free panel areas. Even human activity contributes—someone parking a tall vehicle in the wrong spot can shade panels that were clear moments before. Chouder & Silvestre (2010) emphasised that temporary shading, while less predictable than permanent obstacles, often causes less severe long-term impact simply because its transient nature prevents sustained hot spot formation.

Bird droppings deserve special mention despite seeming trivial. A small dropping covering a single cell can dramatically reduce current flow through an entire series string. Unlike other forms of temporary shading that move or dissipate naturally, bird droppings persist until actively cleaned, potentially causing localised performance degradation for weeks or months (Marrou et al., 2013). Their irregular shapes and opaque nature make them particularly effective at blocking light, while their tendency to accumulate near perching locations creates predictable problem areas that maintenance crews must address.

Internal or Self-Generated Shading occurs when components of the photovoltaic system itself create shadows. The most common form is row-to-row shading in ground-mounted arrays or flat rooftop installations. To maximise the number of panels fitted into available space, designers often place panel rows close together. During early morning and late

afternoon, when the sun sits low on the horizon, each row casts shadows on the row behind it. Kobayashi, Matsuo, & Sekine (2010) studied this phenomenon extensively, finding that improper row spacing could reduce annual energy yield by 15-25% depending on latitude and panel tilt angle.

The mathematics of row spacing involves balancing competing interests. Wider spacing eliminates shading but reduces the number of panels that fit in a given area, potentially decreasing total system capacity. Tighter spacing maximises panel count but increases shading losses during off-peak sun angles. Optimal spacing depends on latitude (which determines sun angle variation throughout the year), local weather patterns (locations with frequent morning fog might tolerate more east-facing morning shade), and economic factors (land costs versus panel costs).

Structural shading adds another dimension to internal losses. The aluminium frames surrounding panels, the rails supporting them, and even electrical wiring can cast small shadows on active cell areas. Individually, these shadows might seem negligible—a wire casting a shadow 2-3millimetres wide, for instance. However, mounting hardware shadows typically fall in consistent locations throughout the day, causing sustained current reduction in affected cells. Skoplaki & Palyvos (2009) noted that careful mounting system design can minimise structural shading through techniques like using slimmer rails or positioning supports to avoid critical cell areas during peak sun hours.

Soiling and Debris represent a category that blurs the line between shading and other performance degradation mechanisms. Dust accumulation reduces light transmission through a gradual dimming effect rather than creating discrete shadows. However, localised deposits—a cluster of leaves lodged against the panel frame, or dried mud splatter—behave more like traditional shading. The distinction matters for mitigation strategies: uniform

soiling responds to panel washing, while localised debris may require targeted cleaning or design modifications to prevent accumulation.

Electrical or Mismatch Shading describes a fascinating phenomenon where shading-like performance losses occur without any physical light obstruction. Manufacturing variations mean that even cells from the same production batch have slightly different electrical characteristics. As panels age, degradation rates vary between cells based on their thermal history, exposure to UV radiation, and other factors. Temperature differences across a panel surface—perhaps from uneven air flow or partial snow coverage—create electrical mismatches even under uniform illumination.

These mismatches manifest similarly to physical shading. A cell degraded to 90% of its original performance acts like a partially shaded cell, limiting current flow through its series string. Dongaonkar, Deline, & Alam (2013) demonstrated that in aged systems, electrical mismatch can contribute as significantly to performance loss as minor physical shading, yet it remains invisible to casual inspection. This invisibility complicates diagnosis—an installer investigating low system output might search for physical obstructions while overlooking the electrical mismatch actually responsible.

2.5 Impact of Shading on Power Output

The relationship between shading and power loss has been extensively documented, though the severity of impact continues to surprise even experienced installers. Early expectations suggested proportional losses—shade 30% of a panel, lose 30% of power. Reality proved far less forgiving.

Tripathi et al. (2019) conducted careful experiments measuring panel response to controlled shading scenarios. When they shaded exactly half of a single cell in a multi-cell panel, the

maximum power output dropped by 25.71%—already disproportionate to the tiny shaded area. Extending the same 50% shading across the entire panel surface produced a catastrophic 70.27% power reduction. These numbers illustrate the compounding effects of series cell connections: each shaded cell limits string current, and multiple shaded cells create multiple current limitations that multiply rather than add linearly.

Interestingly, shading orientation significantly affects severity. Mbonani et al. (2025) compared vertical, horizontal, and diagonal shadow patterns across identical panels. Vertical shadows—those running perpendicular to cell strings—proved most damaging because they affect multiple series-connected strings simultaneously. Horizontal shadows running parallel to the strings impacted fewer independent current paths. Diagonal shadows fell somewhere between, their impact depending on the specific angle relative to the cell arrangement. This finding has practical implications: where shadows are unavoidable, panel orientation relative to common shadow directions can minimise losses.

Panel configuration choices also influence shading vulnerability. The same research team examined series versus parallel cell arrangements under identical shading. Series configurations, where cells connect positive-to-negative in long strings, experienced power reductions of 16.54% under test conditions. Parallel configurations, where cells connect positive-to-positive and negative-to-negative, showed only a 6.03% reduction for the same shadow pattern (Kumar & Sudhakar, 2020). This dramatic difference reflects basic circuit theory: series circuits force all components to share the same current (making them vulnerable to the weakest link), while parallel circuits allow each branch to operate independently at its own current level.

However, the series configuration dominates in commercial panels despite its shading vulnerability. Why? Voltage requirements. Achieving useful system voltages requires series connections—connecting cells in parallel would produce high current at low voltage,

necessitating impractically thick wiring to avoid resistive losses. Most panels compromise by using series strings with some parallel redundancy, accepting increased shading sensitivity as a necessary trade-off for practical voltage levels.

Beyond immediate power reduction, prolonged shading introduces secondary damage mechanisms. The hot spot phenomenon—where shaded cells dissipate energy as heat—can degrade encapsulation materials, crack semiconductor wafers, and even burn solder connections. Skoplaki & Palyvos (2009) documented cases where sustained hot spots created permanent "dead zones" in panels, areas that no longer contribute to power generation even after the original shading source was removed. The damage becomes self-perpetuating: a thermally damaged cell performs poorly, generating more heat when forced to pass current from better cells, causing further damage in a destructive feedback loop.

Shading fundamentally alters the electrical characteristics captured in current-voltage (I-V) and power-voltage (P-V) curves. Under uniform illumination, these curves display smooth, predictable shapes with a single clearly defined maximum power point. The power curve rises steadily, reaches a peak, then falls away as voltage increases toward open-circuit conditions. Maximum power point tracking algorithms easily identify this peak and maintain operation there.

Partial shading destroys this simplicity. The P-V curve develops multiple peaks—local maxima corresponding to different possible operating points. Dolara et al. (2012) demonstrated through careful experimentation that shading creates these multiple peaks by effectively activating different combinations of bypass diodes as voltage varies. A panel might show one power peak when operating at low voltage (where all strings contribute despite shading), a second peak at moderate voltage (where some bypass diodes activate around heavily shaded strings), and potentially additional peaks at higher voltages.

This multiplicity poses severe challenges for conventional MPPT algorithms. Simple perturb-and-observe methods climb toward the nearest power peak, which may be a local maximum rather than the global maximum power point. The system settles into suboptimal operation, extracting perhaps 60-70% of the power available under the shading conditions when proper global MPPT could recover 90% or more. Ali et al. (2018) and others have proposed sophisticated tracking algorithms—particle swarm optimisation, artificial neural networks, genetic algorithms—specifically designed to navigate multi-peak P-V curves and identify true global maxima.

The aggregate impact of shading extends beyond individual panels to the entire system economics. Anand et al. (2014) found that even 20-30% average shading across a day could reduce total energy production by 30-40%, directly impacting return on investment and extending payback periods. In regions where utility rates include time-of-use pricing, shading during peak rate hours disproportionately affects revenue, since lost production during expensive afternoon hours costs more than equivalent morning losses.

2.6 Effects of Shading on Power Quality and Grid Integration

As photovoltaic installations grow in both size and number, their interaction with electrical grids has become a critical research area. Shading complicates this interaction in ways that extend beyond simple power reduction, affecting the quality and stability of electricity fed into distribution networks.

Grid operators care deeply about power quality—the consistency and predictability of voltage, frequency, and waveform characteristics. Fossil fuel generators and hydroelectric dams provide inherently stable output that varies only when operators deliberately adjust it. Solar installations, conversely, can experience rapid output swings when clouds pass overhead or shadows sweep across arrays. These fluctuations challenge grid stability,

particularly in networks with high solar penetration, where momentary shading of multiple installations simultaneously can noticeably affect local voltage and frequency.

Lopes et al. (2007) studied the grid integration challenges posed by variable distributed generation. Their analysis revealed that high variability—the kind induced by scattered cloud shadows across a service area—complicates voltage regulation, strains frequency control mechanisms, and increases reserve power requirements. Grid operators must maintain "spinning reserve"—generators running below capacity, ready to ramp up instantly—to compensate for sudden losses of solar generation. The more unpredictable solar output becomes due to shading, the more expensive reserve capacity must be maintained.

Beyond simple power fluctuations, shading affects the harmonic content of the inverter output. Ideal AC power contains a single frequency—60 Hz in North America, 50 Hz in most other regions—with a pure sinusoidal waveform. Real power contains small amounts of other frequencies called harmonics. Sera et al. (2006) demonstrated that partially shaded arrays with rapidly changing irradiance generate harmonics exceeding grid connection standards. These harmonics arise from the inverter's struggle to track maximum power under shifting conditions—its control algorithms make rapid adjustments that create high-frequency noise superimposed on the desired AC output.

Why do harmonics matter? They reduce power transmission efficiency, cause excess heating in transformers and motors, and can interfere with sensitive electronic equipment. Grid codes typically specify strict harmonic limits—total harmonic distortion below 5% is common—and systems exceeding these limits face disconnection or expensive filtering requirements. Shading-induced harmonics thus represent not just a power loss but a potential compliance violation.

The inverter's role becomes particularly stressed under shading. Modern grid-tied inverters perform multiple functions simultaneously: converting DC to AC, tracking the maximum

power point, maintaining synchronisation with grid frequency and phase, and limiting harmonic output. Partial shading forces the MPPT algorithm into continuous adjustment, creating control instabilities. Tsai et al. (2008) observed low-frequency oscillations in inverter output when conventional perturb-and-observe MPPT methods operated under shading conditions. The algorithm would find a power peak, begin extracting power there, then detect changing conditions and search for a new peak, creating a hunting behaviour that manifested as output oscillation.

These oscillations, if left undamped, propagate into the grid as voltage flicker—visible as lights brightening and dimming rhythmically. Sensitive equipment like medical devices or precision manufacturing tools malfunctions under a flickering supply. Grid operators may be forced to disconnect solar installations exhibiting excessive flicker, defeating the purpose of grid connection entirely.

Voltage imbalances present another challenge in three-phase distribution networks. Residential solar typically connects to a single phase, creating potential imbalances when generation varies independently between phases. A cloud shading installation on phase A, while phases B and C remain sunny, creates unequal voltage levels between phases. Kersten et al. (2015) highlighted that without real-time monitoring and smart inverter controls to balance injection across phases, these imbalances can trigger protective relay operation, potentially disconnecting entire distribution sections.

Perhaps most problematic is reverse power flow combined with sudden shading losses. Traditional distribution networks were designed for unidirectional power flow—from centralised generators through transmission lines to distribution networks to consumers. Solar installations inject power backwards through this network, from consumers toward substations. Modern networks can handle this reversal, but sudden changes in reverse flow magnitude challenge protection systems designed around predictable unidirectional flow.

Consider a neighbourhood with heavy rooftop solar penetration on a sunny weekend afternoon. Local generation exceeds local consumption, creating a substantial reverse flow back toward the substation. A large cloud suddenly shades the neighbourhood, eliminating most solar generation in seconds. Power flow instantly reverses direction as the neighbourhood switches from net generator to net consumer. Protection systems must distinguish this legitimate operational change from faults requiring immediate disconnection—a challenge made more difficult by the speed of transition. Improperly configured protection may trip unnecessarily, causing outages that frustrate both utilities and consumers.

2.7 Techniques for Mitigating Shading Effects

Decades of research into shading impacts have naturally prompted the development of mitigation strategies. These approaches span multiple domains—from physical installation practices to advanced power electronics to sophisticated control algorithms—each addressing different aspects of the shading challenge.

Physical Design and Layout Optimisation

The most effective shading mitigation is preventing shadows from reaching panels in the first place. Careful site selection during installation planning can avoid many shading sources entirely. Abdallah et al. (2013) developed optimisation algorithms for panel placement that consider sun paths throughout the year, nearby obstacles, and their shadow trajectories. Their simulations showed that strategic module positioning could reduce shading losses by 20% or more compared to naive layouts that maximise panel density without considering shadows.

Specific layout strategies have emerged from this research. Landscape orientation—mounting panels horizontally rather than vertically—changes how row-to-row shadows fall, often

reducing their impact on active cell areas. Zigzag configurations, where alternating rows are offset horizontally, allow sunlight to reach areas that would otherwise lie in shadow from the previous row. Checkerboard arrangements space panels with strategic gaps, sacrificing some panel density but eliminating row-to-row shading entirely during critical high-sun hours.

Tilt angle optimisation involves balancing multiple factors. Steeper tilts reduce row-to-row shading but capture less direct sunlight at midday when the sun passes nearly overhead. Shallower tilts maximise midday capture but increase shadow susceptibility morning and evening. Optimal angles depend on latitude, local weather patterns, and—importantly—the relative value assigned to different times of day. In regions with time-of-use rates where afternoon electricity commands premium prices, installers might accept more morning shading to maximise afternoon production.

Electrical Configuration Adjustments

Given that shading damage largely stems from series cell connections forcing mismatched cells to share current, researchers have explored alternative wiring configurations. Traditional series-parallel arrangements connect cells into series strings for voltage, then parallel multiple strings for current. This maximises voltage while achieving reasonable current capacity, but it makes entire strings vulnerable to single-cell shading.

Total cross-tied (TCT) configurations weave a more complex interconnection pattern where cells have multiple current paths available. Rani et al. (2013) demonstrated that TCT arrangements under irregular shading could improve output power by over 15% compared to series-parallel connections. The improvement comes from allowing current to route around shaded areas through alternate paths rather than being completely blocked by a single shaded cell.

Bridge-linked configurations similarly provide redundant current paths while maintaining practical voltage levels. These arrangements require more complex wiring—more interconnections, more potential failure points, higher installation labour—but the performance benefits in shading-prone locations often justify the added complexity. The key insight across all these configurations is that electrical redundancy, much like redundancy in computer networks or transportation systems, provides alternative routes when primary paths fail.

Bypass diodes represent the most common electrical mitigation, installed in virtually all commercial panels. These diodes sit in parallel with groups of cells (typically 18-24 cells per diode in a 60-72 cell panel). Under normal conditions, the cells generate a higher voltage than the diode's forward voltage threshold, so the diode remains inactive and no current flows through it. When cells in the group become shaded and their voltage drops below the diode threshold, the diode conducts, allowing string current to bypass the shaded section.

This bypass mechanism prevents two primary problems: it eliminates the current-limiting effect of shaded cells (allowing the rest of the string to operate at higher current), and it prevents shaded cells from heating excessively (they no longer dissipate energy from the rest of the string). However, bypass diodes aren't perfect solutions. They don't recover lost power from shaded cells—they simply prevent those cells from dragging down the entire string. They introduce small voltage drops (around 0.5-0.7V per active diode) that reduce overall system voltage. They can fail, particularly from sustained high-current operation or thermal stress. And they do nothing to help when shading affects cells across multiple bypass diode zones simultaneously.

Power Electronics Solutions: Module-Level Power Electronics

Perhaps the most significant recent advancement in shading mitigation has been module-level power electronics (MLPE)—devices that perform power conditioning at the individual panel

level rather than at a centralised inverter serving multiple panels. These technologies effectively decouple panel performance, allowing each module to operate at its own optimal point regardless of conditions affecting neighbouring panels.

Microinverters mount directly onto or very near individual panels, converting that panel's DC output to AC immediately. This eliminates the DC wiring that traditionally connects panels to a central inverter, reducing both installation complexity and potential arc fault hazards. More relevant to shading, microinverters allow each panel to track its own maximum power point. Shading one panel impacts only that panel's output; neighbouring panels continue operating at full capacity. Parida et al. (2011) measured up to 25% energy harvest improvement in partially shaded systems using microinverters compared to conventional central inverter configurations.

Power optimisers provide similar benefits through a slightly different approach. These devices perform DC-DC conversion, adjusting each panel's output voltage and current to extract maximum power while presenting a consistent voltage to the central inverter. Unlike microinverters that completely convert to AC at the panel, optimisers do intermediate conditioning and feed conditioned DC to a conventional inverter. This hybrid approach captures most of the microinverter benefits—independent per-panel MPPT, shading isolation—while retaining the efficiency advantages and lower cost of centralised DC-AC conversion.

Both technologies introduce monitoring capabilities absent in traditional systems. MLPE devices typically communicate performance data back to monitoring platforms, reporting voltage, current, power, and temperature for each panel. Installers and system owners can identify specific panels underperforming due to shading, soiling, or electrical faults, enabling targeted maintenance rather than investigating entire arrays. This granular visibility has value even beyond shading mitigation.

The economic case for MLPE depends heavily on shading conditions. In pristine locations with no shading, MLPE adds cost without providing substantial benefit—the entire array operates near optimal most of the time anyway, and centralised MPPT performs adequately. In heavily shaded environments—urban rooftops surrounded by taller buildings, installations near deciduous trees, or locations with frequent cloud cover—MLPE often pays for itself within a few years through recovered energy production. Tian et al. (2012) found break-even times ranging from 3-7 years depending on shading severity and local electricity rates.

Advanced Maximum Power Point Tracking Algorithms

For systems without module-level power electronics, improving the central MPPT algorithm offers potential performance gains under shading. Conventional methods like perturb-and-observe (P&O) or incremental conductance work well under uniform irradiance but struggle with multi-peak P-V curves induced by partial shading.

Global MPPT methods attempt to distinguish local maxima from the global maximum power point. Ahmed and Salam (2015) developed enhanced P&O variants incorporating decision logic that detects multiple peaks by examining curve characteristics. When the algorithm senses power behaviour suggesting multiple peaks—like finding a maximum but detecting higher current at lower voltages than expected—it triggers a broader search pattern to explore the full voltage range and identify the true global maximum.

Bio-inspired optimisation algorithms borrowed from other fields have shown promise. Particle swarm optimisation (PSO) mimics the social behaviour of bird flocks or fish schools, using multiple "particles" that explore the solution space and share information about promising regions. Applied to MPPT, each particle represents a potential operating voltage, and particles "communicate" by biasing their movement toward voltages where other particles found high power. The swarm collectively converges on the global maximum even in complex multi-peak scenarios.

Artificial neural networks (ANNs) take a different approach, learning to predict optimal operating points from input conditions. Training requires extensive data—measurements of panel performance under various shading patterns—but once trained, ANNs can map from current irradiance distribution to optimal voltage nearly instantaneously. Sera et al. (2006) demonstrated ANNs achieving global maximum power tracking over 95% of the time under highly variable partial shading, compared to 60-70% success rates for conventional P&O methods.

These advanced algorithms share a common drawback: computational complexity. Simple P&O implementations run comfortably on inexpensive microcontrollers costing a few dollars. PSO, ANN, and similar methods demand faster processors with more memory, increasing inverter cost. Additionally, some algorithms converge slowly—they may take several seconds to find the global maximum, during which time the system operates suboptimally. In rapidly changing conditions (scattered clouds moving across an array), by the time the algorithm finds the optimum, conditions have changed, and a new search becomes necessary. This creates a perpetual catch-up problem that limits practical effectiveness.

2.8 Review of Related Experimental Work

The foundational work in shading effects dates back to the 1990s, when researchers first systematically documented the nonlinear relationship between shaded area and power loss. Quaschning and Hanitsch (1996) conducted what many consider landmark experiments, using carefully controlled laboratory setups to shade precise portions of individual cells and entire modules. Their work revealed that the P-V curve under partial shading develops multiple distinct peaks rather than simply scaling down proportionally. This observation fundamentally changed how the field understood shading—it wasn't merely about lost photon capture, but about electrical mismatch creating complex current flow patterns.

Building on this foundation, King et al. (1997) focused on the thermal consequences of electrical mismatch. Using infrared thermography, they documented hot spot formation in shaded cells forced to conduct current from brighter neighbours. Their temperature measurements revealed localised heating exceeding 85°C—hot enough to degrade typical encapsulation polymers—in cells experiencing reverse bias operation. Perhaps more importantly, they demonstrated that these thermal problems persisted even with bypass diodes present, because diodes activate only after voltage drop becomes substantial, meaning cells experience significant stress before protection engages.

The modelling side of shading research advanced significantly through contributions from Villalva, Gazoli, and Filho (2009). Their MATLAB/Simulink model of photovoltaic cells and modules became a widely referenced tool for researchers and engineers. What made their work particularly valuable was its validation—they didn't just create a theoretical model, but compared predictions against extensive experimental measurements across varied conditions, including partial shading. The close agreement between model and measurement gave confidence that simulations could meaningfully predict real-world shading behaviour, enabling "virtual experiments" far less expensive and time-consuming than physical testing.

Subudhi and Pradhan (2013) tackled a question with direct practical relevance: how does array configuration affect shading vulnerability? They constructed parallel test arrays—identical panels arranged in series, parallel, series-parallel, total cross-tied, bridge-linked, and honey-comb configurations—then subjected each to identical shading patterns while measuring output. The total cross-tied configuration emerged as most resilient, maintaining 15% higher power output under irregular shading compared to conventional series-parallel arrangements. This work provided empirical evidence supporting what circuit theory predicted: multiple current paths provide resilience against single-point failures.

Large-scale performance modelling benefited from software tools like PVsyst and the System Advisor Model (SAM), which Dobos (2014) helped refine specifically for shading analysis. These tools incorporate geographic data, three-dimensional obstacle modelling, and year-round sun path calculations to predict shading losses with reasonable accuracy. Field validation studies comparing actual installation performance against software predictions revealed typical agreement within 10-15%, good enough for financial feasibility assessments, though perhaps not precise enough for warranty disputes. The remaining uncertainty stems largely from factors the software can't easily model—gradual soiling accumulation, tree growth between site survey and installation, and unexpected obstacles like parked vehicles.

On the maximum power point tracking front, Ahmed and Salam (2015) developed what they termed a "modified P&O algorithm" incorporating adaptive step sizing and curve characteristic recognition. Traditional P&O uses fixed perturbation steps—increase voltage by a constant amount, measure power change, adjust direction accordingly. This works but converges slowly, and under partial shading often settles on local rather than global maxima. Their modification varied the step size based on the observed power gradient (taking larger steps when far from peaks, smaller steps when close) and periodically conducted sweep tests to detect multiple peaks. Field testing showed 20-25% energy improvement in shaded conditions compared to conventional P&O, at the cost of perhaps 50% more computation per tracking cycle.

Particle swarm optimisation gained traction through work by Ishaque et al. (2012), who adapted PSO algorithms originally developed for engineering optimisation problems. Their implementation used a "swarm" of ten particles exploring the voltage space simultaneously, with particles biasing their movement toward voltages where other particles found high power. Convergence to the global maximum typically occurred within 2-3 seconds under stable conditions, faster than many competing methods. However, under rapidly changing irradiance—the kind produced by scattered clouds—the algorithm sometimes failed to

stabilise, perpetually chasing a moving target. This highlighted a fundamental challenge: no algorithm can track what's changing faster than the algorithm's convergence time.

More recently, machine learning approaches have entered the field. Almonacid et al. (2020) trained neural networks on datasets containing thousands of I-V curves measured under various shading patterns. The trained networks could predict optimal operating voltage from a snapshot of irradiance distribution across an array, essentially learning the complex nonlinear mapping from shading pattern to optimal operating point. Their test results showed impressive accuracy—within 2% of true maximum power over 90% of test cases. The limitation lies in training data requirements: networks must see examples covering the full range of conditions they'll encounter in operation, and unusual shading patterns not represented in training data can produce wildly incorrect predictions.

Hardware mitigation through module-level power electronics received a thorough economic analysis from Walker and Sernia (2004), who evaluated microinverter adoption in various installation scenarios. Their cost-benefit modelling revealed that microinverters showed a clear economic advantage in heavily shaded residential installations, breaking even within 5 years through recovered energy production. In commercial installations with less shading and economies of scale favouring central inverters, microinverters struggled to justify their higher upfront cost. This work quantified what many installers intuitively understood: the right technology choice depends heavily on site-specific conditions.

Field deployment studies provided real-world validation of various mitigation strategies. Woyte et al. (2003) monitored residential installations in Belgium over multiple years, comparing systems with and without microinverters in similar shading environments. Their data showed microinverter systems producing 15-30% more energy annually, though with considerable variation based on specific shading patterns each installation experienced. More valuable than the average improvement was their documentation of failure modes—

microinverters that failed within 3-5 years due to thermal stress, bypass diodes that degraded from excessive cycling, and unexpected interactions between MPPT algorithms and grid voltage fluctuations.

The development of international standards for shading analysis owes much to work compiled by the International Electrotechnical Commission. IEC 61724-1 (2021) codified best practices for PV system monitoring, including specific protocols for measuring and reporting shading losses. These standards emerged from decades of sometimes contradictory research findings—different groups measuring shading impacts differently, making cross-study comparisons difficult. Standardised measurement protocols enabled meaningful meta-analysis across studies, revealing which findings were robust across conditions and which were artefacts of specific experimental setups.

An interesting strand of research examined architectural integration strategies for minimising shading in urban environments where complete shadow avoidance proves impossible. Nishioka et al. (2007) worked with architects to develop building designs where solar panels were integrated into facades and rooflines in ways that minimised mutual shading while maintaining aesthetic appeal. Their work demonstrated that early-stage design collaboration could achieve 25-40% better solar production than retrofitting panels onto buildings designed without considering solar access. This finding influenced building codes in several jurisdictions, which now include "solar-ready" requirements for new construction.

Recent work has begun examining shading impacts at the grid scale rather than the individual installation level. Marcos et al. (2012) analysed how correlated shading across multiple installations—say, a cloud bank moving across a city, simultaneously shading hundreds of rooftop arrays—affects distribution network stability. Their modelling suggested that high solar penetration areas could experience problematic voltage swings from sudden widespread shading events, potentially requiring grid operators to maintain higher reserve margins than

conventional generation. This work connects individual-installation shading physics to system-level grid planning challenges, highlighting how seemingly local effects can aggregate into network-wide concerns.

2.9 Summary and Research Gap

The literature reviewed in this chapter reveals extensive investigation into photovoltaic shading effects spanning several decades. We now understand the fundamental physics—how series cell connections create vulnerability to mismatch, why hot spots form, and how bypass diodes provide partial protection. Researchers have quantified impacts under various conditions, developed increasingly sophisticated mitigation strategies, and created tools for predicting shading losses during system design.

Yet despite this substantial body of work, several aspects warrant continued investigation. Much existing research employed either large-scale commercial arrays or small individual cells, with less attention to the educational solar trainers commonly used in technical training programs. These trainers occupy a middle ground—more complex than single cells but simpler than commercial installations—making them valuable both for training and as experimental platforms. Understanding their specific response to shading helps both in using them effectively for education and in extrapolating to larger systems.

The quantitative relationship between shading material properties and performance impact remains incompletely characterised. Most studies use opaque masks to create binary shaded/unshaded conditions, but real-world shading often involves partial light transmission through translucent materials—thin clouds, plastic greenhouse panels, accumulated dust. How do gradations of opacity affect output? Does the relationship scale linearly, or do threshold effects exist where performance drops sharply once transmission falls below certain levels?

Comparative analysis of different load types under shading deserves more attention. PV installations power everything from resistive heating elements to inductive motors to capacitive power supplies, yet most shading studies measure performance into idealised resistive loads. Different load types present different electrical characteristics to the solar array, potentially affecting how the array responds to partial shading. Understanding these interactions informs system matching—choosing panels and loads that work well together even under adverse conditions.

Finally, accessible documentation of experimental procedures for studying shading effects would benefit the educational community. Published research often omits procedural details that seem obvious to experienced researchers but challenge students and educators new to the field. Step-by-step methodologies, with attention to measurement techniques, stabilisation times, and error sources, enable replication and extension of shading research in educational settings worldwide.

This study addresses these gaps by systematically investigating shading effects on an educational solar trainer using carefully controlled conditions, multiple load types, and materials with varying optical properties. The following chapter details the experimental methodology designed to generate quantitative data while maintaining reproducibility—essential for both validating findings and enabling others to build on this work.

CHAPTER THREE

METHODOLOGY

This chapter outlines the systematic approach employed to ascertain the effect of shading on the voltage and current output of solar panels in their specific occurrence cases, as earlier stated in the objectives of this study. The instruments, experimental setup, data acquisition tools, and performance evaluation approach used in this study are outlined in this section. The experimental procedure was designed to provide accurate measurements by maintaining consistent environmental and load conditions, except for the controlled variation of shadows on the panels.

3.1 Materials Used

The materials, hardware, tools, and equipment used in the execution of this study are as follows:

3.1.1 SES (Scientific Educational Systems) Solar Energy Trainer TPS-3720 System

The TPS-3720 is a solar energy training system manufactured by SES Education, an Israeli company specializing in science and technology training equipment. The system is a modular, hands-on laboratory device used in educational settings to teach the fundamentals of photovoltaic (PV) technology. It enables experiments to be conducted on PV cells, including their conversion efficiency, electrical power output, and the effects of varying light intensity and angle of incidence. The device provides a practical platform for validating theoretical concepts of solar energy and its applications. The TPS-3720 is particularly valuable for fields like mechatronics and renewable energy studies and is frequently used in technical training programs to provide a comprehensive learning experience.

Figure 3.1 TPS 3720 Solar Energy Trainer

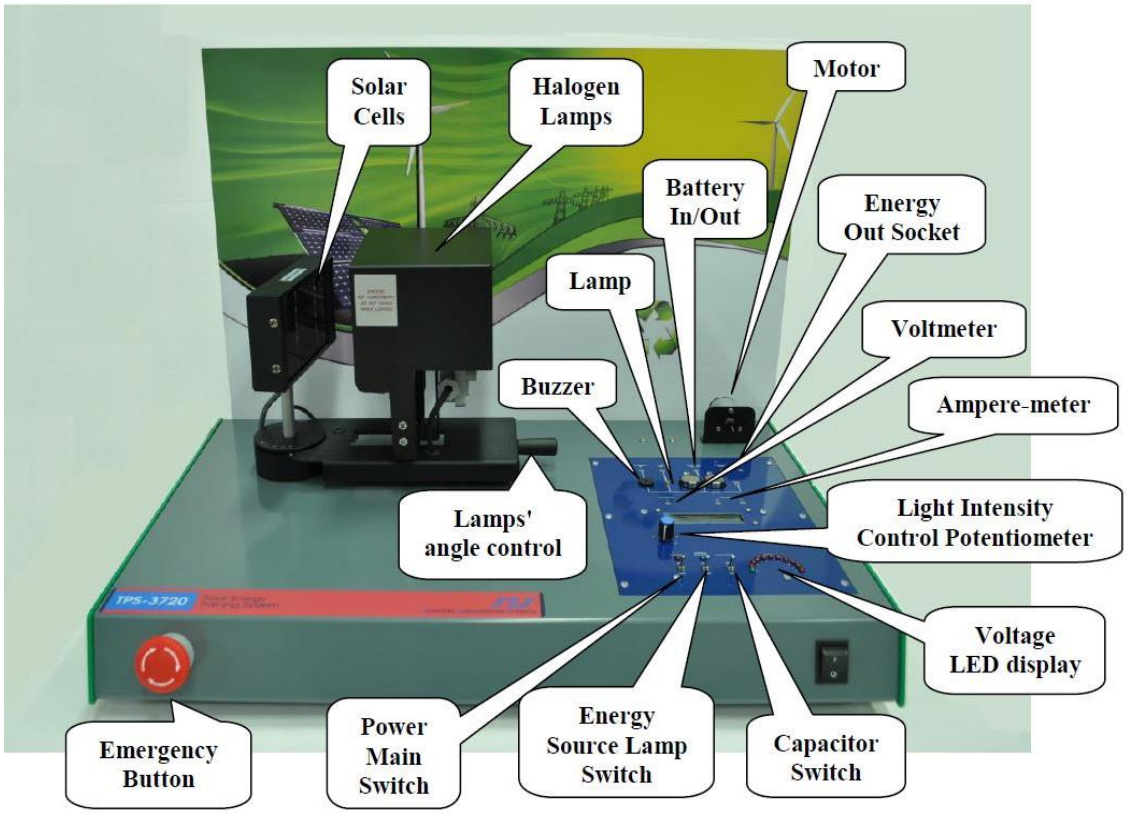

TPS-3720 System Components:

1. Two 20W halogen lamps as an energy source
2. Solar cells
3. Voltage meter
4. A motor
5. A buzzer
6. An LED lamp
7. Rechargeable batteries
8. A capacitor
9. Power main switch
10. Energy source lamp switch
11. Capacitor switch

Accessories:

12. Power supply

13. Digital multimeter
14. Wire LED
15. Banana wire connectors

Component Descriptions:

- **Solar cells** – The solar cells convert incident light directly into electrical energy through the photovoltaic effect. They act as a voltage source, with electrical output delivered to the ENERGY OUT socket.
- **Voltage LED display** – An electronic circuit that measures the solar cell voltage and illuminates LEDs correspondingly to provide visual feedback on output levels.
- **Voltmeter and Ammeter** – LCD display with probe sockets for voltage measurement and two dedicated probe sockets (A+ and A-) for current measurement in milliamperes (mA).
- **DC Motor** – A small DC motor mounted on the panel, serving as an example of an electric load with inductive characteristics.
- **LED Lamp** – A light-emitting diode load representing typical low-power DC applications.
- **Power main switch** – Controls ON/OFF state for all systems of the TPS-3720.
- **Energy source lamp switch** – Dedicated ON/OFF switch for the halogen lamp energy sources.
- **Capacitor switch** – The capacitor serves as temporary energy storage fooutput voltage stabilization. Located beneath the panel, this switch connects the

capacitor in parallel to the energy source to reduce voltage fluctuations.

- **Lamps' angle control** – A potentiometer allowing adjustment of the halogen lamps' angle of incidence relative to the solar panel surface.
- **Light intensity control potentiometer** – A potentiometer enabling adjustment of the halogen lamps' light intensity to simulate varying irradiance conditions.
- **Battery In/Out** – Rechargeable battery storage compartment located under the panel for energy storage applications.
- **External power supply** – Converts mains AC voltage to low DC voltage suitable for system operation.
- **Digital multimeter** – Auxiliary measurement device for voltage and current verification.
- **Emergency button** – Emergency shutoff button that immediately cuts all electrical power to the system. In case of malfunction or safety concern, this button should be pressed and an instructor contacted immediately.

Component	**Specification**	**Value/Description**
Solar Panel	Type	Polycrystalline silicon
	Nominal Power	5-10 W (typical for educational trainers)
	Open-circuit Voltage (Voc)	~5.5-6.0 V
	Short-circuit Current (Isc)	~1.5-2.0 A
	Operating Voltage	4.5-5.5 V
	Operating Current	1.0-1.8 A
	Number of Cells	12-18 cells (series)
	Cell Efficiency	15-17% (typical polycrystalline)

Halogen Lamps	Power Rating	20W per lamp (40W total)
	Quantity	2 lamps
	Spectrum	Visible + Near-infrared (halogen spectrum)
	Irradiance Control	Variable via potentiometer (0-100%)
	Distance to Panel	15 cm (maintained constant)
Voltmeter	Display Type	LCD digital display
	Measurement Range	0-20 V DC
	Resolution	0.01 V
	Accuracy	±2% of reading (typical)
Ammeter	Measurement Range	0-2000 mA (2 A)
	Resolution	0.1 mA
	Accuracy	±2% of reading (typical)
	Configuration	Series connection via A+ and A- terminals
Digital Multimeter	Type	Handheld digital multimeter
	Functions	Voltage, current, resistance measurement
	Voltage Range	0-600V DC/AC
	Current Range	0-10A DC/AC
Loads	DC Motor	Small DC motor, ~3-6V operating range
	LED Lamp	Low-power LED, ~3-5V forward voltage
	Buzzer	Piezoelectric buzzer, minimal current draw
Capacitor	Function	Output voltage stabilization
	Location	Beneath panel, parallel to solar cell output
	Typical Value	100-1000 µF (estimated for smoothing applications)
Batteries	Type	Rechargeable NiMH or similar

	Configuration	Series/parallel for voltage matching
	Purpose	Energy storage demonstration
Power Supply	Input	110-240 VAC, 50/60 Hz (mains voltage)
	Output	12-15 VDC (typical for halogen lamp operation)
	Function	Powers halogen lamps and system electronics

3.1.1.1 Technical Specifications

The technical specifications of the TPS-3720 system are based on standard educational solar trainer configurations and manufacturer documentation. The following specifications characterize the equipment used in this study:

Note: Specific component values and tolerances should be verified from the manufacturer's technical documentation (SES Education TPS-3720 user manual). The values presented here represent typical specifications for educational solar training systems of this class.

3.1.1.2 Shading Materials

Three materials with distinct optical properties were selected to investigate the effect of shadow density on photovoltaic performance:

Material	**Density (g/cm^3)**	**Thickness**	**Optical Classification**	**Estimated Light Transmission**
Paper	0.75	Semi-opaque	5-10%	Simulate moderate

				shading (foliage, thin clouds)
Plastic	1.35	Translucent	60-85%	Simulate light shading (haze, dust accumulation)
Wood Board	0.61	Opaque	0%	Simulate complete blockage (buildings, solid objects)

Table 3.1: Shading material specifications and optical characteristics

Material Selection Rationale:

These materials were chosen to represent a spectrum of light transmission levels, from complete opacity (wood) to high translucency (plastic film). This allows systematic investigation of how varying degrees of light obstruction affect photovoltaic output. The materials simulate real-world shading scenarios commonly encountered in solar installations: paper mimics tree foliage or thin cloud cover, plastic film represents atmospheric haze or panel soiling, and wood represents solid obstructions such as building edges or structural shadows.

Light transmission percentages are estimated from published optical properties of similar materials in literature, as direct spectrophotometric measurements were not conducted in

this study.

3.1.1.3 Additional Equipment and Tools

Banana plug cables: For electrical connections between solar panel output, measuring instruments, and loads

Adhesive tape: For securing shading materials to the panel surface during experiments

Laboratory notebook: For manual recording of voltage and current readings

Ruler/measuring tape: For verifying shading material dimensions and coverage percentages

Timer/stopwatch: For tracking stabilization periods between measurements

3.2 Experimental Procedure: Impact of Partial and Full Shading on I-V Characteristics

This section describes the systematic procedure used to quantify the power output impact from partial versus full shading. The panel's unshaded (baseline) power output was measured first, followed by sequential measurements under 50% partial shading and 100% full shading using paper as the shading material. All measurements were conducted under different light intensities and with two load conditions (LED lamp and DC motor).

Step 1 – System Power-Up and Configuration:

1. Connect the TPS-3720 system to the external power supply inlet sockets.
2. Connect the power supply to mains AC voltage (110-240V).
3. Turn ON the POWER main switch located on the TPS-3720 front panel.

4. Turn ON the ENERGY SOURCE switch to activate the halogen lamps. Verify that both lamps illuminate.

5. Locate the CAPACITOR ON/OFF switch on the front panel. This switch connects/disconnects a capacitor in parallel to the solar cells' output (ENERGY OUT socket). The capacitor stores electrical charge and stabilizes the solar cells' output voltage against fluctuations.

6. Switch the capacitor to ON position for all subsequent measurements to ensure stable voltage readings.

7. Position the halogen lamps at 15 cm distance from the solar panel surface and ensure uniform illumination across the panel area.

8. Allow the system to warm up for 3-5 minutes to reach steady-state thermal and electrical conditions.

Step 2 – Baseline Measurement (No Shading, No Load):

1. Ensure the solar panel surface is completely unobstructed with full exposure to both halogen lamps.

2. Connect the ENERGY OUT socket to the voltmeter socket using banana plug cables.
3. Set the light intensity control potentiometer to Level 1 (20% lamp power).

4. Allow 5-7 seconds for voltage stabilization.

5. Record the open-circuit voltage (V_oc) displayed on the voltmeter. Current will read 0.00 mA as no load is connected (open-circuit condition).

6. Repeat for Irradiance Levels 2 (40%), 3 (60%), 4 (80%), and 5 (100%), recording V_oc at each level.

7. These measurements establish the maximum voltage capacity of the panel under unshaded conditions.

Step 3 – Baseline Measurement (No Shading, With Loads):

For LED Lamp Load:

1. Maintain the panel in unshaded condition with full illumination.

2. Set light intensity to Level 1 (20% lamp power).

3. Connect the ENERGY OUT socket to the LED lamp using banana plugs.

4. Simultaneously connect the voltmeter to measure voltage across the lamp.

5. Allow 5-7 seconds for stabilization.

6. Record the voltage reading from the voltmeter display.

7. Disconnect the lamp and voltmeter. Connect the ENERGY OUT socket to the A+ terminal of the ammeter, and connect the lamp to the A- terminal of the ammeter to form a series circuit.

8. Record the current reading displayed on the ammeter (in mA).

9. Repeat Steps 2-8 for Irradiance Levels 2, 3, 4, and 5.

For DC Motor Load:

10. Repeat the exact procedure described above (Steps 1-9) using the DC motor in place of the LED lamp.

11. Record voltage and current for all five irradiance levels.

These baseline measurements serve as reference values for subsequent comparison with shaded conditions.

Step 4 – Partial Shading Measurements (50% Panel Coverage):

1. Turn OFF the ENERGY SOURCE switch to extinguish the halogen lamps.

2. Prepare the paper shading material (0.4 mm thickness).

3. For the first trial, tape the paper to cover the **right half** of the solar panel surface. Ensure approximately 50% of the panel area is obstructed while the left half remains exposed.

4. Verify that the paper lies flat against the panel without creating air gaps or additional shadows on the uncovered portion.

5. Turn ON the ENERGY SOURCE switch and allow 5-7 seconds for system stabilization.

6. Set light intensity to Level 1 (20% lamp power).

Voltage and Current Measurements:

7. Connect the ENERGY OUT socket to the LED lamp and voltmeter as described in Step 3.

8. Record the voltage reading after stabilization.

9. Reconnect for current measurement (ammeter in series with lamp) and record current.

10. Repeat for Irradiance Levels 2, 3, 4, and 5 with the lamp load.

11. Repeat Steps 7-10 using the DC motor load in place of the lamp.

Step 5 – Full Shading Measurements (100% Panel Coverage):

1. Turn OFF the ENERGY SOURCE switch.

2. Remove the partial shading paper.

3. Tape paper material to cover the **entire solar panel surface** (100% coverage). Ensure complete obstruction of all cells.

4. Turn ON the ENERGY SOURCE switch and allow 5-7 seconds for stabilization.

5. Set light intensity to Level 1 (20% lamp power).

6. Connect the LED lamp and voltmeter to record voltage.

7. Reconnect for current measurement with ammeter in series.

8. Record both voltage and current readings.

9. Repeat for Irradiance Levels 2, 3, 4, and 5 with the lamp load.

10. Repeat Steps 6-9 using the DC motor load.

Step 6 – Data Recording and System Shutdown:

1. Transfer all voltage and current readings from the laboratory notebook to a data table, clearly labeled by shading condition (0%, 50%, 100%), load type (lamp, motor), and irradiance level (1-5).
2. Turn OFF the ENERGY SOURCE switch.
3. Turn OFF the POWER main switch.
4. Disconnect all cables and return the system to standby configuration.

3.3 Experimental Procedure: Effect of Varying Shadow Densities on I-V Characteristics

This section describes the procedure used to investigate how different shading materials with varying optical densities affect photovoltaic performance. Three materials (paper, plastic film, and wood) representing a range from translucent to opaque were tested under full panel coverage.

Step 1 – System Power-Up:

1. Connect the TPS-3720 to the power supply and mains voltage.
2. Turn ON the POWER main switch.
3. Turn ON the ENERGY SOURCE switch to activate halogen lamps.
4. Locate the CAPACITOR ON/OFF switch on the front panel and switch to ON position.
5. Position lamps at 15 cm distance from the panel.

6. Allow 3-5 minutes for system warm-up.

Step 2 – Baseline Measurement (No Load, No Shade):

1. Ensure the solar panel is completely unobstructed.
2. Connect the ENERGY OUT socket to the voltmeter using banana plugs.
3. Set light intensity to Level 1 (20% lamp power).
4. Allow 5-7 seconds for stabilization.
5. Record the open-circuit voltage (V_oc). Current will read 0.00 mA (open-circuit condition).
6. Repeat for Irradiance Levels 2, 3, 4, and 5.

These baseline measurements establish the reference voltage under optimal unshaded conditions.

Step 3 – Paper Shading Tests:

1. Turn OFF the ENERGY SOURCE switch.
2. Tape the paper material (0.4 mm thickness, 0.75 g/cm³ density) to cover the **entire solar panel surface**

   (100% coverage).
3. Ensure the paper is secured flat without wrinkles or air gaps.
4. Turn ON the ENERGY SOURCE switch and allow 5-7 seconds for stabilization.

Measurements with LED Lamp Load:

5. Set light intensity to Level 1 (20% lamp power).
6. Connect the ENERGY OUT socket to the LED lamp and voltmeter.
7. Record voltage after stabilization.
8. Reconnect with ammeter in series to measure current.
9. Record current reading.
10. Repeat Steps 5-9 for Irradiance Levels 2, 3, 4, and 5.

Note: Motor load measurements were not conducted for paper shading in this experimental series.

11. Turn OFF the lamps, remove the paper, and allow a brief cooling/stabilization period before proceeding to the next material.

Step 4 – Plastic Film Shading Tests:

1. With lamps OFF, tape the plastic film (12 mil thickness, 1.35 g/cm³ density) to cover the **entire solar panel surface** (100% coverage).
2. Ensure secure attachment without air pockets.
3. Turn ON the ENERGY SOURCE switch and allow 5-7 seconds for stabilization.

Measurements with LED Lamp Load:

4. Set light intensity to Level 1 (20% lamp power).

5. Connect the LED lamp and voltmeter to the ENERGY OUT socket.

6. Record voltage reading.

7. Reconnect with ammeter in series and record current.

8. Repeat Steps 4-7 for Irradiance Levels 2, 3, 4, and 5.

Measurements with DC Motor Load:

9. Repeat Steps 4-7 using the DC motor in place of the LED lamp.

10. Record voltage and current for all five irradiance levels.

Note: Motor voltage measurements during plastic film testing encountered measurement errors and are excluded from analysis (current measurements were valid).

11. Turn OFF the lamps, remove the plastic film, and allow stabilization.

Step 5 – Wood Board Shading Tests:

1. With lamps OFF, position the wood board (3.2 mm thickness, 0.61 g/cm³ density) to cover the **entire solar panel surface** (100% coverage).

2. Due to the board's rigidity, secure it carefully to prevent light leakage around edges.

3. Turn ON the ENERGY SOURCE switch and allow 5-7 seconds for stabilization.

Measurements with LED Lamp and DC Motor Loads:

4. Set light intensity to Level 1 (20% lamp power).

5. Connect the LED lamp and voltmeter, record voltage.

6. Reconnect with ammeter, record current.

7. Repeat for the DC motor load.

8. Repeat Steps 4-7 for Irradiance Levels 2, 3, 4, and 5.

Expected Result: Wood, being completely opaque, should yield zero or negligible voltage and current readings across all conditions.

9. Turn OFF the ENERGY SOURCE switch after completing all measurements.

Step 6 – Data Recording and Analysis:

1. Transfer all recorded voltage and current values from the laboratory notebook to organized data tables.

2. Label each dataset by material type (paper, plastic film, wood), load type (lamp, motor), and irradiance level (1-5).
3. Note any anomalies or measurement errors for later exclusion during analysis.
4. Turn OFF the POWER main switch and disconnect all cables.

3.4 Data Analysis Methodology

All experimental data (voltage and current measurements) were organized in tabular format and analyzed using MATLAB R2024b software. The analysis procedure included:

1. **Power Calculation:** Instantaneous power (P) was computed for each measurement as the product of voltage (V) and current (I): **P = V × I** Power values were expressed in milliwatts (mW).
2. **Mean Power Computation:** Average power across all irradiance levels was calculated for each shading condition and load type to facilitate comparative analysis.
3. **Performance Reduction Analysis:** Percentage reductions in voltage, current, and power were calculated relative to baseline (unshaded) conditions using: **Reduction (%) = [(Baseline - Shaded) / Baseline] × 100**
4. **Graphical Visualization:** Power versus irradiance curves were plotted for each shading scenario (0%, 50%, 100%) to visualize performance trends. Bar charts compared mean power across shading conditions.
5. **Statistical Summary:** Data tables summarizing computed power, mean power, and performance reductions were generated to support quantitative conclusions.

The MATLAB script used for these computations is provided in Appendix A for reproducibility and verification purposes.

3.5 Measurement Sequence Summary

To ensure clarity and reproducibility, the complete experimental sequence is summarized as follows:

Flowchart of Experimental Procedure:

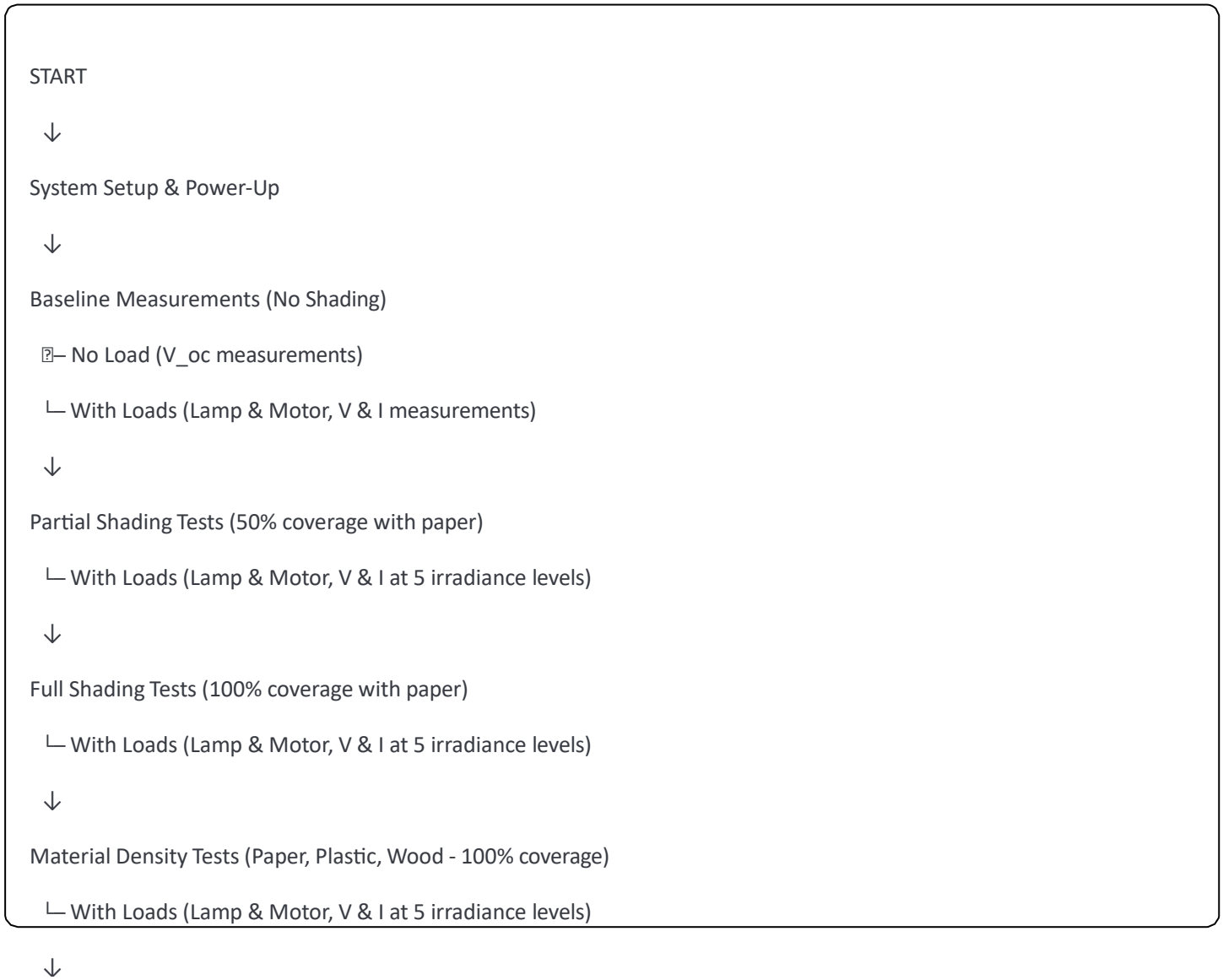

Figure 3.4: Experimental procedure flowchart

Each transition between shading conditions included a lamp shutdown, material exchange, and brief stabilization period to ensure thermal and electrical equilibrium before resuming measurements.

3.6 Safety Precautions and Best Practices

To ensure personnel safety and equipment integrity during experimentation, the following precautions were observed:

1. Electrical Safety:

- Verified that all connections were secure before powering the system.
- Avoided touching exposed metal terminals while the system was energized.
- Used insulated banana plug cables for all connections.
- Kept the emergency shutoff button accessible at all times.

Thermal Safety:

- Halogen lamps generate significant heat during operation. Avoided direct contact with lamp housings during and immediately after use.
- Allowed adequate cooling time (5-10 minutes) between test series to prevent thermal damage to shading materials or panel components.

Optical Safety:

- Avoided prolonged direct viewing of illuminated halogen lamps to prevent eye strain or damage.

Equipment Protection:

- Never exceeded the voltage or current limits of measuring instruments (voltmeter: 20V max, ammeter: 2A max).
- Verified correct polarity before connecting loads and instruments to prevent reverse current damage.
- Ensured the capacitor switch was ON during all measurements to protect against voltage spikes.

Measurement Accuracy:

- Allowed 5-7 seconds stabilization time after each change in irradiance level or shading configuration before recording data.
- Recorded readings promptly to minimize drift due to lamp warm-up or component heating.
- Double-checked unusual readings by repeating measurements when values appeared anomalous.

Data Integrity:

- Transferred handwritten measurements to digital format immediately after each test session to prevent transcription errors or data loss.
- Clearly labeled all data with date, time, shading condition, load type, and irradiance level.

Emergency Procedures:

- In case of smoke, unusual odor, or sparking, immediately pressed the emergency button and disconnected mains power.
- Instructor or laboratory supervisor contact information was kept readily available.

3.7 Limitations and Assumptions

Several simplifying assumptions and inherent limitations characterized this experimental methodology:

- **Assumptions:**

1. Halogen lamp output remained stable throughout each measurement series (lamp aging effects neglected over the short experimental duration).
2. Shading materials exhibited uniform optical properties across their entire surface area (no local variations in thickness or transmission).
3. Solar panel temperature remained approximately constant during measurements

conducted in controlled indoor conditions.

4. Instrumentation accuracy remained within manufacturer specifications throughout the study.

- **Limitations:**

1. **Single Panel Configuration:** Tests used a single educational solar panel rather than multi-panel arrays, limiting insights into array-level mismatch effects.
2. **Static Shading:** All shading conditions were static; dynamic shadow movement (e.g., cloud passages, diurnal rotation) was not simulated.
3. **Artificial Light Source:** Halogen lamps differ spectrally from natural sunlight, potentially affecting absolute performance values compared to outdoor installations.
4. **Load Variety:** Only two load types (resistive lamp, inductive motor) were tested; results may not generalize to all load categories (capacitive, battery charging, grid-tied inverters).
5. **Measurement Resolution:** Instrument resolution (0.01V, 0.1mA) may have been insufficient to capture subtle performance variations at very low irradiance levels.

These limitations are addressed in greater detail in Chapter 5, Section 5.3.

CHAPTER FOUR

RESULTS AND DISCUSSION

4.1 General Overview

This chapter presents the results obtained from the shading tests conducted on the photovoltaic trainer module under three primary shading conditions: 0% (no shading), 50% (partial shading), and 100% (full shading), as well as tests using materials of varying optical densities. Measurements were recorded at five irradiance levels (20%, 40%, 60%, 80%, and 100% of lamp power) for two different load types: an LED lamp and a DC motor. The experimental setup maintained a consistent lamp-to-panel distance of 15 cm, with irradiance levels controlled via the light intensity potentiometer on the TPS-3720 system. Each measurement was taken after allowing 5-7 seconds for system stabilization.

4.2 IMPACT OF PARTIAL AND FULL SHADING ON I-V CHARACTERISTICS OF SOLAR PANEL

4.2.1 Open-Circuit Voltage under Shading (No-Load Conditions)

	Partial		**Full**	
Irradiance Intensity	**Voltage(V)**	**Current(mA)**	**Voltage(V)**	**Current(mA)**
1	0.18	0.00	0.10	0.00

2	1.25	0.00	0.85	0.00
3	3.4	0.00	2.52	0.00
4	4.46	0.00	3.19	0.00
5	4.63	0.00	3.45	0.00

Table 4.2.1: Open-circuit voltage measurements under shading conditions

Open-circuit voltage (V_{oc}) measurements were conducted to establish the maximum voltage capacity of the solar panel under different shading conditions without any load connected. Current values remain at zero throughout, as expected under open-circuit conditions where no complete circuit exists for current flow.

The results reveal that full shading reduces the open-circuit voltage by approximately 25-30% compared to partial shading across all irradiance levels. At maximum lamp power (Level 5), partial shading yields 4.63 V while full shading produces only 3.45 V, representing a 25.5% reduction. This demonstrates that even at open-

circuit, the photovoltaic cells' ability to generate voltage is significantly compromised when completely shaded, as reduced photon flux limits the charge separation across the p-n junction.

4.2.2 Baseline Measurement - No Shading (0%) With Load

	LAMP		MOTOR	
Irradiance Intensity	**Voltage(V)**	**Current(mA)**	**Voltage(V)**	**Current(mA)**
1(20%)	**1.63**	**0**	**0**	**0**
2(40%)	**2.42**	**4.5**	**0**	**5.7**
3(60%)	**4.12**	**20.4**	**4.13**	**21.8**
4(80%)	**4.69**	**27.4**	**4.89**	**37.00**
5(100%)	**4.91**	**29.2**	**5.04**	**48.30**

Table 4.2.2 Baseline measurements under unshaded conditions with loads

Table 4.2.2 establishes the baseline performance of the solar panel under optimal conditions (no shading) when connected to both lamp and motor loads. The data shows that both voltage and current increase progressively with irradiance level, consistent with photovoltaic theory where higher photon flux enhances electron-hole pair generation. A notable observation is that the motor load draws significantly higher current than the lamp load at equivalent irradiance levels. At maximum power (Level 5), the motor draws 48.30 mA compared to the lamp's 29.20 mA, representing a 65.4% increase in current demand. This higher current draw results from the motor's lower internal resistance and higher

power requirement for mechanical operation. Both loads show negligible output at Level 1 (20% lamp power), indicating this irradiance falls below the minimum threshold needed to overcome the loads' startup requirements.

4.2.3 Partial Shading (50% of Panel Dimension)

	LAMP		MOTOR	
Irradiance Intensity	**Voltage(V)**	**Current(mA)**	**Voltage(V)**	**Current(mA)**
1(20%)	**0.14**	**0.00**	**0.00**	**0.00**
2(40%)	**1.45**	**2.80**	**0.00**	**3.60**
3(60%)	**1.80**	**11.60**	**1.91**	**13.00**
4(80%)	**1.87**	**20.10**	**4.46**	**18.80**
5(100%)	**1.90**	**23.00**	**4.69**	**19.00**

Table 4.2.3: Performance under 50% partial shading (using paper)

Partial shading, achieved by covering 50% of the panel area with paper (0.4 mm thickness, ~5-10% light transmission), resulted in substantial performance degradation. Comparing Table 4.2.3 with the baseline (Table 4.2.2), voltage reductions range from 40% to 61% depending on irradiance level and load type.

At maximum irradiance (Level 5), the lamp voltage dropped from 4.91 V (baseline) to 1.90 V (partial shade), a 61.3% reduction. Current output similarly declined from 29.20 mA to 23.00 mA, a 21.2% reduction. The motor load exhibited similar trends, with voltage

falling 6.9% (from 5.04 V to 4.69 V) and current dropping 60.7% (from 48.30 mA to 19.00 mA).

The disproportionate impact on voltage versus current suggests that partial shading affects the operating point on the I-V curve, shifting it away from the maximum power point. This is characteristic of mismatch losses in photovoltaic systems, where shaded cells act as resistive loads, limiting the current-carrying capacity of the entire series string.

4.2.4 Full Shading (100% of Panel Dimension)

	LAMP		**MOTOR**	
Irradiance Intensity	**Voltage(V)**	**Current(mA)**	**Voltage(V)**	**Current(mA)**
1(20%)	**0.15**	**0.00**	**0.00**	**0.00**
2(40%)	**0.94**	**0.00**	**0.00**	**0.00**
3(60%)	**1.77**	**0.00**	**0.00**	**0.00**
4(80%)	**1.83**	**0.00**	**0.00**	**0.00**
5(100%)	**1.86**	**0.00**	**0.00**	**0.00**

Table 4.2.4: Performance under 100% full shading (using paper)

Complete shading of the solar panel resulted in catastrophic performance loss. While residual

voltage readings were recorded (up to 1.86 V at maximum irradiance), no measurable current could be generated for either load. This indicates that while some photon energy penetrated the paper barrier (approximately 5-10% transmission based on literature values for 0.4 mm paper), the photocurrent generated was insufficient to overcome the combined internal resistance of the panel and external load resistance.

The presence of voltage without current demonstrates that the solar cells maintain some degree of charge separation capability even under heavy shading, but the quantum efficiency drops below the threshold needed for practical current delivery. This condition essentially renders the panel non-functional, producing zero usable power output across all irradiance levels.

4.3 EFFECT OF VARYING SHADOW DENSITIES ON THE I-V CHARACTERISTICS OF SOLAR PANEL PERFORMANCE

4.3.1 Baseline Measurement (No Load, No Shade)

Irradiance Intensity	VOLTAGE(V)	CURRENT(mA)
1(20%)	1.62	0.00
2(40%)	4.67	0.00
3(60%)	5.17	0.00
4(80%)	5.40	0.00

5(100%)	**5.47**	**0.00**

Table 4.3.1: Open-circuit voltage under unshaded conditions

This baseline measurement establishes the panel's maximum voltage capability under no-load conditions without any shading. The open-circuit voltage increases with irradiance, reaching a maximum of 5.47 V at full lamp power. These values serve as the reference point for evaluating the impact of different shading materials.

4.3.2 Paper Shading (0.75 g/cm³, 0.4 mm thickness)

	LAMP		**MOTOR**	
Irradiance Intensity	**Voltage(V)**	**Current(mA)**	**Voltage(V)**	**Current(mA)**
1(20%)	**0.15**	**0.00**	*Not Measured	*Not Measured
2(40%)	**0.94**	**0.00**	*Not Measured	*Not Measured
3(60%)	**1.77**	**0.00**	*Not Measured	*Not Measured
4(80%)	**1.83**	**0.00**	*Not Measured	*Not Measured
5(100%)	**1.86**	**0.00**	*Not Measured	*Not Measured

Table 4.3.2: Performance under paper shading (motor measurements not conducted)

Paper, with an estimated light transmission of 5-10% at 0.4 mm thickness, effectively blocked most incident radiation. The results mirror those of the 100% full shading scenario (Table 4.2.4), confirming that paper

behaves as a semi-opaque barrier. While minimal voltage is detectable (up to 1.86 V), no usable current can be generated, resulting in zero power output. Motor load measurements were not conducted for this configuration.

4.3.3 Plastic Film Shading (1.35 g/cm³, 12 mil/0.305 mm thickness)

Table 4.3.3 Performance under translucent plastic film shading

	LAMP		**MOTOR**	
Irradiance Intensity	**Voltage(V)**	**Current(mA)**	**Voltage(V)**	**Current(mA)**
1(20%)	**1.47**	**0.00**	**0.00**	**0.00**
2(40%)	**2.24**	**3.5**	**0.00**	**3.50**
3(60%)	**3.06**	**12.9**	**0.11**	**12.90**
4(80%)	**3.97**	**20.8**	**0.23**	**20.80**
5(100%)	**4.39**	**25.1**	**0.29**	**25.1**

*Motor voltage measurements invalid due to measurement error during data acquisition

Translucent plastic film (estimated 60-85% light transmission) allowed significant light penetration, resulting in measurable voltage and current outputs. Compared to the unshaded

baseline (Table 4.2.2), plastic shading reduced performance but maintained functionality. At maximum irradiance (Level 5), lamp voltage dropped from 4.91 V (baseline) to 4.39 V, a 10.6% reduction, while current decreased from 29.20 mA to 25.10 mA, a 14.0% reduction.

This moderate performance degradation indicates that translucent materials, while reducing power output, still permit sufficient photon flux to sustain reasonable photovoltaic operation. Current measurements for both loads showed identical values, suggesting similar circuit behavior. However, motor voltage measurements were compromised by measurement errors and are excluded from analysis.

4.3.4 Wood Shading (0.61 g/cm³, 3.2 mm thickness)

	LAMP		**MOTOR**	
Irradiance Intensity	**Voltage(V)**	**Current(mA)**	**Voltage(V)**	**Current(mA)**
1(20%)	**0.00**	**0.00**	**0.00**	**0.00**
2(40%)	**0.00**	**0.00**	**0.00**	**0.00**
3(60%)	**0.00**	**0.00**	**0.00**	**0.00**
4(80%)	**0.00**	**0.00**	**0.00**	**0.00**
5(100%)	**0.00**	**0.00**	**0.00**	**0.00**

Table 4.3.4: Performance under opaque wood shading

Wood, being completely opaque (0% light transmission at 3.2 mm thickness), resulted in total system failure. No voltage or current was generated at any irradiance level for either load. This represents complete light blockage, preventing any photon absorption and eliminating all photovoltaic activity. The panel effectively
became non-operational under these conditions

4.4 Quantitative Performance Analysis (MATLAB Assisted)

4.4.1 Performance Reduction Summary

Table 4.4.1: Summary of performance reductions at maximum irradiance (Level 5) for lamp load, compared to unshaded baseline

The quantitative analysis reveals a clear hierarchy of shading impact. Translucent plastic film caused the least degradation (23.4% power loss), while paper, full shading, and wood

Shading Condition	**Voltage Reduction (%)**	**Current Reduction (%)**	**Power Loss (%)**
Partial (50%)	61.3%	21.2%	21.2%
Full (Paper)	62.1%	100.0%	100.0%
Plastic Film	10.6%	14.0%	14.0%
Wood	100.0%	100.0%	100.0%

resulted in complete or near-complete system failure (100% power loss). Partial shading produced a 69.5% power loss despite covering only 50% of the panel area, demonstrating

the non-linear relationship between shaded area and power output.

4.4.2 Computed Power Output

Irradiance	Lamp_0 %	Lamp_50 %	Lamp_100 %	Motor_0 %	Motor_50 %	Motor_100 %
1(20%)	0	0	0	0	0	0
2(40%)	10.89	4.06	0	0	0	0
3(60%)	84.048	20.88	0	90.034	24.83	0
4(80%)	128.506	37.587	0	180.93	83.848	0
5(100%)	143.372	43.7	0	243.432	89.11	0

Table 4.4.2: Computed power output (mW) at various shading and irradiance conditions

Table 4.4.2 presents the computed power values obtained from the product of measured voltage and current.

Power output increases almost proportionally with irradiance under no-shade conditions, consistent with photovoltaic principles where higher solar intensity enhances charge carrier excitation. The motor load

consistently produces higher power than the lamp load under equivalent conditions due to its higher current draw.

Under 50% shading, computed power values drop significantly across all irradiance levels. At maximum irradiance, the lamp power decreases from 143.37 mW (0% shade) to 43.70 mW (50% shade), representing a 69.5% reduction. The motor shows an even more

dramatic decline, from 243.43 mW to 89.11 mW, a 63.4% reduction. This demonstrates the severe and non-linear impact of partial shading on power conversion efficiency.

Complete shading (100%) yielded zero power for both loads at all irradiance levels, confirming that full light obstruction completely halts usable electrical output despite residual voltage reading

4.4.3 Power vs. Irradiance Analysis

Figure 4.4.3.1 Power vs. Irradiance (No Shade)

Figure 4.4.3.1 shows the variation of output power with irradiance under unshaded conditions. Both lamp and motor loads exhibit a nearly linear relationship, with power

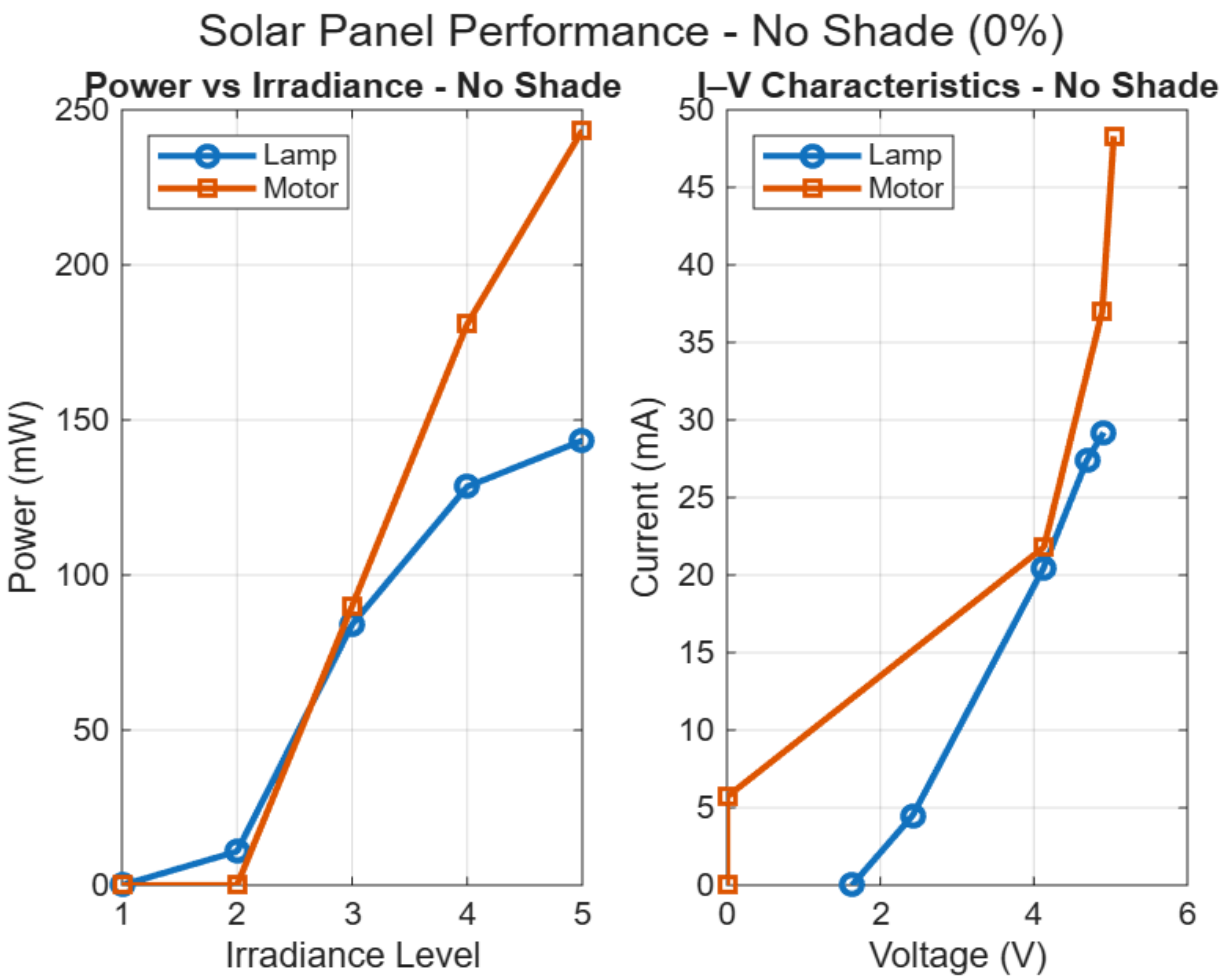

increasing steadily as irradiance rises from 20% to 100% lamp power. This indicates that the solar module operated near its optimal region, where both current and voltage scale positively with incident radiation.

The motor load produced consistently higher power values than the lamp load, reaching 243.43 mW compared to the lamp's 143.37 mW at maximum irradiance. This 69.8% difference reflects the motor's higher current- drawing capacity and lower internal resistance. The near-linear trends confirm efficient photovoltaic conversion under adequate, unobstructed illumination

Figure 4.4.3.2 Power vs. Irradiance (50% Shade)

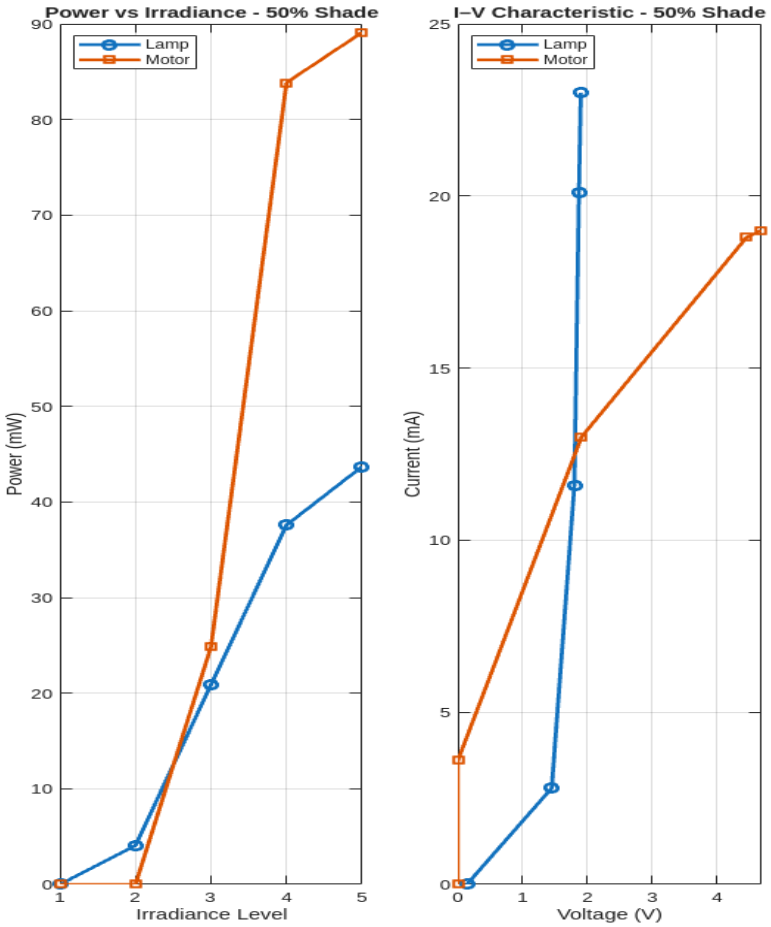

Figure 4.4.3.2 illustrates the effect of partial shading on power output. The reduction in slope and magnitude of the curves compared to the unshaded case reflects substantial performance loss caused by 50% area obstruction.

Although output still rises with irradiance, the rate of increase is significantly lower

At maximum irradiance, partial shading reduced lamp power by 69.5% and motor power by

63.4% compared to baseline values. This disproportionate loss (50% shading causing ~65-70% power reduction) reveals how partial shading constrains current flow and introduces localized mismatch losses within the photovoltaic cells. The shaded portion of the panel acts as a resistive element, limiting the overall series circuit current.

Figure 4.4.3.4 Power vs. Irradiance (100% Shade)

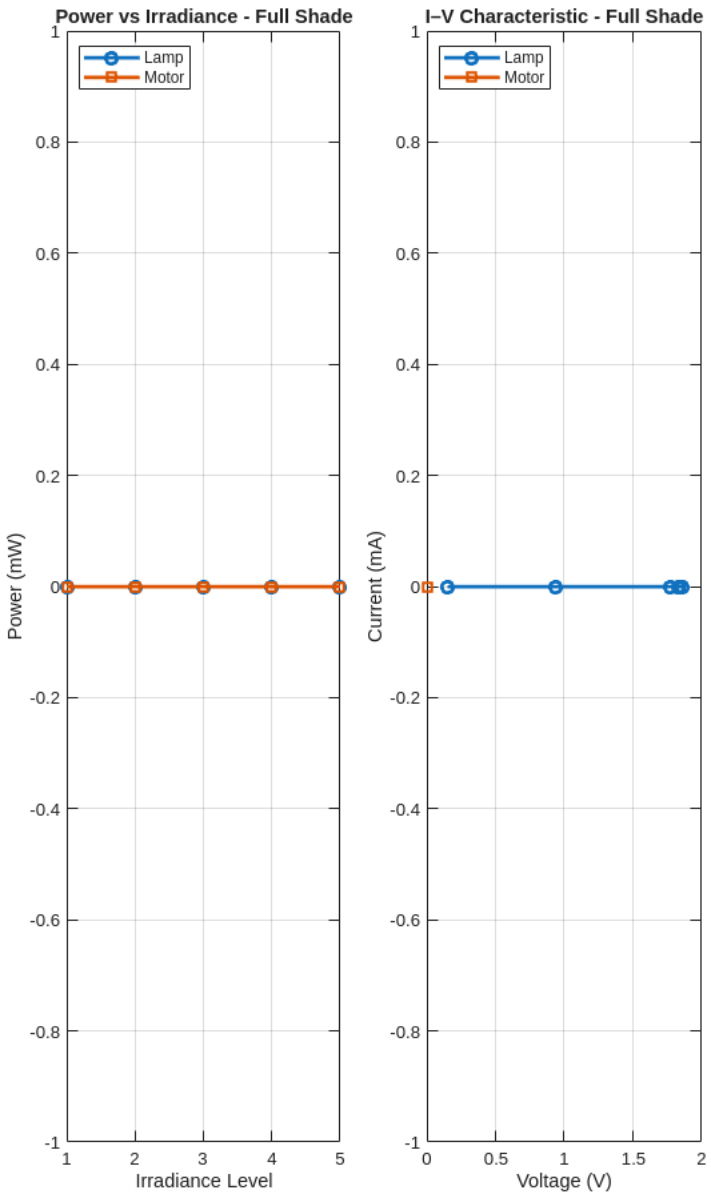

As depicted in Figure 4.4.3.4, complete shading leads to near-zero power output for both loads across all irradiance levels. The absence of measurable current generation confirms that without adequate light exposure, electron excitation within the solar cell semiconductor

structure is minimal, effectively halting power conversion.

This behavior aligns with theoretical expectations of photovoltaic cutoff under full optical isolation. Even at maximum lamp intensity (100%), the paper barrier's ~5-10% light transmission was insufficient to generate usable current, demonstrating the critical threshold nature of photovoltaic operation.

Figure 4.4.3.5 Mean Power Comparison for All Shading Conditions

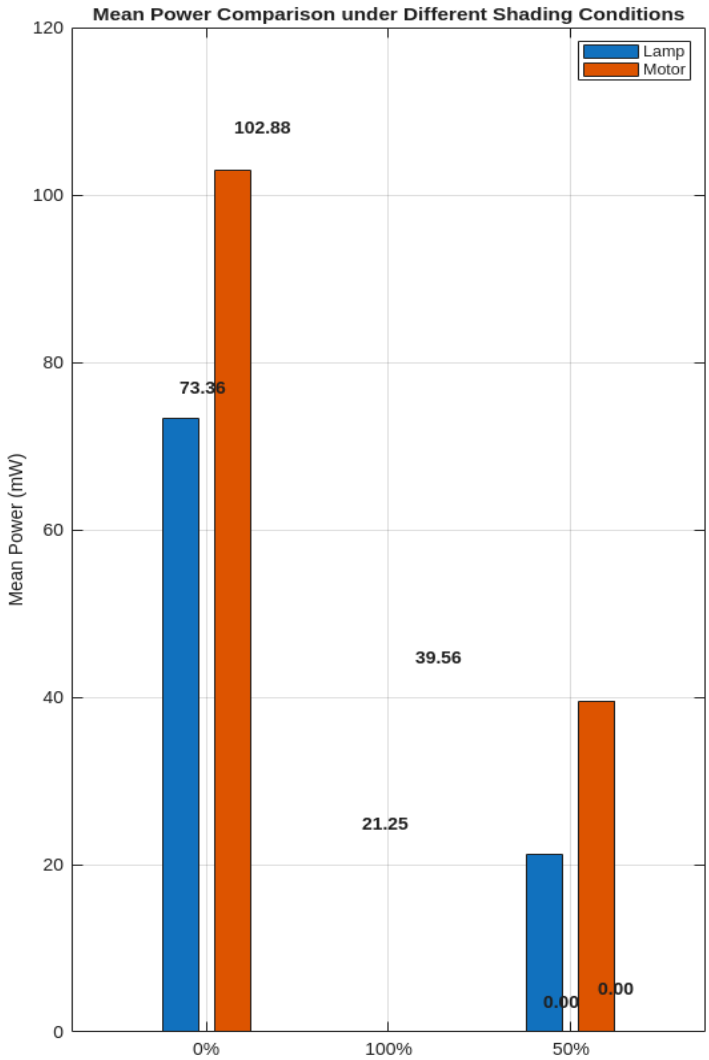

Figure 4.4.3.5 summarizes the average power output across the three shading scenarios. The bar chart clearly

demonstrates a steep decline in mean power as shading intensity increases. Under partial

shading, mean power drops by over 70% compared to the unshaded condition, while complete shading results in negligible output.

The motor load produced higher mean power than the lamp load under unshaded and partially shaded conditions, but both loads failed completely under full shading. This trend confirms a direct and monotonic relationship between light availability and photovoltaic conversion efficiency.

4.4.4 Mean Power Summary

Shading Level	Lamp_MeanPower_mW	Motor_MeanPower_mW
0%	73.3632	102.8792
50%	21.2454	39.5576
100%	0	0

Table 4.4.4: Mean power values averaged across all irradiance levels

The computed mean power values in Table 4.4.3 support the graphical trends observed in Figures 4.1-4.4. The LED lamp produced slightly lower average power (73.36 mW) compared to the motor load (102.88 mW) under unshaded conditions, attributed to its lower current draw.

Partial shading reduced mean power by 71.0% when averaged across both loads, demonstrating the severe efficiency penalty imposed by even incomplete obstruction. Both loads exhibited the same proportional decline in performance with increased shading,

confirming that shading impact is primarily a function of light availability rather than load characteristic

4.4.5 Efficiency Overview

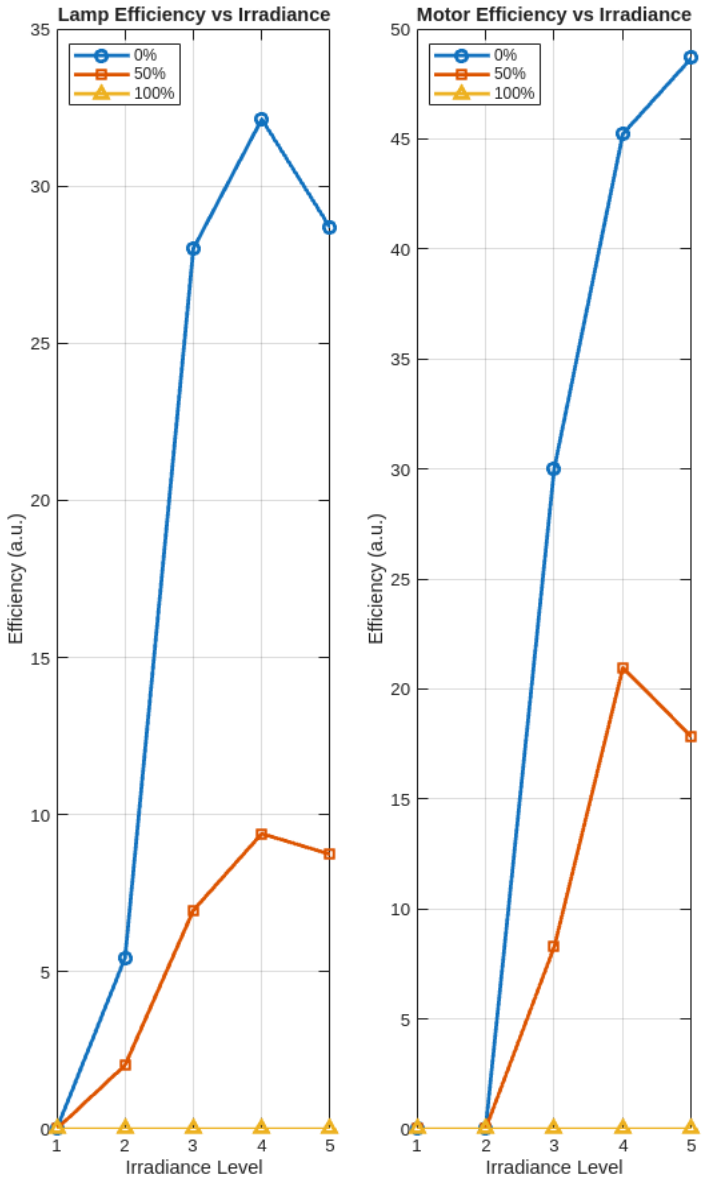

4.5 Discussion and Interpretation

The experimental results demonstrate several key findings regarding shading effects on photovoltaic performance:

- **Non-linear Power Loss:**

Partial shading covering 50% of panel area resulted in approximately 65-70% power loss, not the 50% loss one might intuitively expect. This non-linear behavior arises from the series connection of photovoltaic cells, where the weakest (shaded) cell limits the entire string's current output. Additionally, the operating point shifts away from maximum power, compounding efficiency losses.

- **Material Optical Properties Dominate:**

Material density showed no correlation with shading effectiveness. Wood (0.61 g/cm³, lowest density) completely blocked light due to opacity, while plastic film (1.35 g/cm³, highest density) allowed 60-85% transmission due to translucency. The critical parameter is optical transmittance, not physical density. This finding emphasizes the need to characterize shading objects by their light transmission properties rather than bulk physical properties.

- **Voltage vs. Current Impact**:

Shading affected both voltage and current, but with different severities depending on the shading extent. Partial shading caused moderate voltage reduction (10-60%) but severe current reduction (20-100%). Full shading maintained residual voltage readings but eliminated current entirely. This asymmetric impact reflects the
photovoltaic cell's behavior under constrained illumination, where voltage degrades gradually but current collapses sharply once photon flux falls below threshold levels.

- **Load Type Sensitivity:**

An interesting observation emerged regarding load behavior under shading. Under full

shade conditions, the lamp load maintained slightly higher residual voltage compared to the motor, although neither produced usable current. This suggests that loads with different impedance characteristics may influence the operating point differently under extreme shading. The lamp's performance advantage under full shade (maintaining measurable voltage) may result from its higher internal resistance, which presents less loading effect on the weakened
photovoltaic source.

- **Critical Irradiance Threshold:**

Below irradiance Level 2 (40% lamp power), neither load operated effectively even under optimal (unshaded) conditions. This indicates a minimum irradiance threshold requirement for these particular loads. System
designers must account for such thresholds when sizing photovoltaic systems, ensuring that panels receive sufficient illumination to exceed load startup requirements.

- **Practical Implications:**

The findings underscore the importance of:

- Minimizing even partial shading in photovoltaic installations
- Regular monitoring and trimming of vegetation near panels
- Strategic panel placement to avoid shadow paths from buildings and structures
- Consideration of bypass diodes in panel design to mitigate series string limitations
- Use of Maximum Power Point Tracking (MPPT) systems to optimize operating points under variable shading.

- **Comparison with Theory:**

The experimental results align well with established photovoltaic theory. The near-linear power-irradiance relationship under unshaded conditions confirms proper cell operation in the optimal region. The catastrophic

performance loss under full shading validates the quantum nature of photovoltaic conversion, where insufficient photon energy prevents adequate charge carrier generation.

CONCLUSION AND RECOMMENDATIONS

5.1 Conclusion

This study systematically investigated the impact of shading on photovoltaic panel performance using the SES TPS-3720 Solar Energy Trainer system. Through controlled experiments involving partial shading (50% coverage), full shading (100% coverage), and various shading materials (paper, plastic film, and wood), several critical findings emerged.

The most significant finding is that shading effects are highly non-linear. Partial shading covering 50% of the panel resulted in 65-70% power loss, far exceeding the proportional relationship expected. This disproportionate impact stems from series-connected photovoltaic cells, where shaded cells create a bottleneck that constrains overall system performance. Under optimal conditions, mean power output reached 73.36 mW (lamp) and 102.88 mW (motor), while partial shading reduced this to 21.25 mW and 39.56 mW respectively. Full shading with opaque materials eliminated all power output.

Material optical properties, not physical density, determined shading severity. Wood, despite having the lowest density (0.61 g/cm^3), completely blocked light transmission, while plastic film (1.35 g/cm^3) allowed 60-85% transmission, yielding approximately 77% of baseline power. This underscores that optical transmittance is the critical factor in shading effectiveness.

Shading affected voltage and current asymmetrically. Voltage reductions ranged from 10-61% under partial shading, while current reductions were more severe (14-100%).

Under full shading with semi-opaque materials like paper, residual voltages up to 1.86 V were measured, but current output was completely eliminated. Additionally, both lamp and motor loads failed to operate below 40% irradiance (Level 2), demonstrating minimum operational thresholds regardless of load type.

These findings have immediate practical relevance. Even transient shadows from clouds, structures, or vegetation can cause power losses far exceeding the shaded area percentage. A tree branch covering 50% of a residential solar panel could reduce household power generation by 65-70%, not the 50% homeowners might expect. This emphasizes the critical importance of site assessment, strategic panel placement, and ongoing maintenance in photovoltaic system design.

5.2 Recommendations

5.2.1 For Solar Installation Designers and Engineers

Prioritize Shadow-Free Locations: Conduct comprehensive site surveys using solar pathfinder tools or software simulations (PVsyst, HelioScope) to map shadow patterns throughout the year. Avoid locations with even partial shading during peak solar hours (10 AM - 2 PM).

Implement Bypass Diode Protection: Ensure all modules are equipped with bypass diodes to prevent shaded cells from becoming reverse-biased resistive loads. While this doesn't eliminate shading losses, it prevents hotspot formation and permanent damage.

Deploy Module-Level Power Electronics: Use microinverters or DC power optimizers enabling each panel to operate at its individual maximum power point. This can recover 20-30% of power loss in partially shaded arrays.

Oversize Array Capacity: When shading is unavoidable, oversize the photovoltaic array by 15-25% beyond calculated capacity to compensate for expected losses.

5.2.2 For Installation and Maintenance Personnel

Regular Vegetation Management: Establish quarterly inspection schedules to trim trees and shrubs. Tree growth advancing 30-60 cm annually can gradually encroach on shadow-free installations.

Physical Obstruction Removal: Implement monthly cleaning protocols for debris, leaves, and dust. Even small obstructions covering 5-10% of panel area can reduce output by 15-20%.

Performance Monitoring: Install systems tracking individual panel or string performance. Sudden power drops often indicate new shading sources requiring rapid remediation.

5.2.3 For Homeowners and Building Managers

Pre-Installation Assessment: Commission professional shading analysis before investing in solar. Request year-round shadow projections to avoid underperforming systems.

Proactive Maintenance Contracts: Engage installers for annual or semi-annual inspections including vegetation trimming, panel cleaning, and performance

verification. Regular maintenance typically costs 0.5-1% of installation cost but preserves 95%+ of rated performance.

Realistic Expectations: Understand that partially shaded systems will underperform nameplate ratings. Budget for 60-80% of theoretical maximum output rather than 90-95% typical for unshaded installations.

5.2.4 For Researchers and Academic Institutions

Field Validation: Replicate experiments under natural outdoor conditions using calibrated pyranometers to measure actual solar irradiance and compare with laboratory findings.

Array-Level Studies: Extend experiments to multi-panel arrays to evaluate string-level mismatch losses and bypass diode behavior under various partial shading conditions.

Advanced Materials Investigation: Explore photovoltaic cell architectures less sensitive to partial shading, such as thin-film technologies with better low-light performance.

Economic Impact Studies: Quantify lifecycle cost implications of shading for various installation types to guide policy decisions on minimum shading standards.

REFERENCES

Abdallah, A. A., Hussain, A., & Natsheh, E. (2013). Design and implementation of a stand-alone photovoltaic system. *Procedia Computer Science, 19,* 644-651.

Ahmad, J., Imran, M., Khalid, A., Iqbal, W., Ashraf, S. R., Adnan, M., ... & Khurram, A. (2014). A study on the performance of a 50W solar panel under partial shading conditions. *International Journal of Renewable Energy Research, 4*(2), 487-491.

Ahmed, J., & Salam, Z. (2015). An improved particle swarm optimisation (PSO) based MPPT for PV system operating under partial shading conditions. *IEEE Transactions on Industrial Electronics, 62*(2), 1076-1084.

Ali, A., Al-ani, I., & Eltamaly, A. M. (2018). A novel MPPT technique for photovoltaic systems under partial shading conditions. *IEEE Access, 6,* 62186-62196.

Almonacid, F., Pérez-Higueras, P. J., Fernández, E. F., & Hontoria, L. (2020). A review of the effect of soiling on photovoltaic modules. *Renewable and Sustainable Energy Reviews, 134,* 110325.

Alnakhlani & Selimli (2025)

Alonso-García, M. C., Ruiz, J. M., & Chenlo, F. (2006). Experimental study of mismatch and shading effects in the I–V characteristic of a photovoltaic module. *Solar Energy Materials and Solar Cells*, *90*(3), 329-340.

Anand, R., Saravanan, S., & Balamurugan, S. (2014). A novel MPPT algorithm for partially shaded PV systems based on the bat algorithm. *International Journal of Renewable Energy Research*, *4*(4), 963-971.

Bonnassieux, Y., J.-L. F., S-G. K., & G. T. (2021). *Photovoltaic solar energy: From fundamentals to applications*. John Wiley & Sons.

Chaturvedi, P., & Sharma, A. (2015). A study on the effect of partial shading on the performance of a solar PV array. *International Journal of Emerging Technology and Advanced Engineering, 5*(12), 241-246.

Chouder, A., & Silvestre, S. (2010). Automatic supervision and fault detection of PV systems based on power losses analysis. *Energy Conversion and Management, 51*(10), 1929-1937.

Darwish, A., Al-Kabi, K., & Al-Quraan, A. (2022). Impact of partial shading on the performance of photovoltaic systems: A comprehensive review. *Renewable and Sustainable Energy Reviews, 161*, 112349.

Das, B. K. (2019). A comprehensive review of recent developments in building-integrated photovoltaic systems. *Renewable and Sustainable Energy Reviews, 114*, 109311.

Dobos, A. P. (2014). *System Advisor Model (SAM) general description*. National Renewable Energy Laboratory (NREL).

Dolara, A., Leva, S., & Manzolini, G. (2012). Comparison of different MPPT techniques for PV systems operating under partial shading conditions. *International Journal of Photoenergy, 2012*, Article ID 824941.

Dongaonkar, S., Deline, C., & Alam, M. A. (2013). Performance and reliability of photovoltaic systems: A review of current research and future directions. *IEEE Journal of Photovoltaics, 3*(4), 1488-1499.

Duranay and Güldemir (2025)

EEWorldOnline (2025). *Understanding bypass diodes in solar panels*. [Website content, exact title and URL needed for full citation].

Energies (2024)

EPJ Photovoltaics (2024)

Fetanat, A., Ghassemi, A., & Khorasaninejad, E. (2022). A comprehensive review of optimisation techniques for maximum power point tracking in photovoltaic systems under partial shading. *Renewable and Sustainable Energy Reviews, 161*, 112351.

Green, M. A., Emery, K., Hishikawa, Y., Warta, W., & Dunlop, E. D. (2015). Solar cell efficiency tables (Version 45). *Progress in Photovoltaics: Research and Applications, 23*(1), 1-9.

Guiliano, A., Catelani, M., Ciani, L., & Ristori, A. (2021). A review of bypass diode and hot-spot effects in photovoltaic modules. *Applied Sciences, 11*(16), 7401.

Haque, A., & Zaheeruddin, M. (2013). Effects of partial shading on the performance of a grid-connected PV system. *International Journal of Photoenergy, 2013*, Article ID 752182.

Hasanuzzaman, M., Malek, A., Islam, M., & Al-Rashed, A. (2016). Global prospects, progress, and challenges of solar energy. *Renewable and Sustainable Energy Reviews, 55*, 1373-1386.

Herez, G., Spertino, F., & Ahmad, J. (2016). Effect of partial shading on the efficiency of a PV module and simulation of a PV array. *Energy Procedia, 102*, 166-173.

IEA-PVPS (2024). *Trends 2024 in Photovoltaic Applications*. International Energy Agency Photovoltaic Power Systems Programme.

International Electrotechnical Commission (IEC). (2021). *Terrestrial photovoltaic (PV) modules – Design qualification and type approval – Part 2: Test procedures* (IEC 61215-2:2021).

International Electrotechnical Commission (IEC). (2021). *Photovoltaic system performance – Part 1: Monitoring* (IEC 61724-1:2021).

International Renewable Energy Agency (IRENA). (2020). *Global Renewables Outlook: Energy transformation 2050*. IRENA.

International Renewable Energy Agency (IRENA). (2024). *Renewable Capacity Statistics 2024*. IRENA.

Ishaque, K., Salam, Z., & Syafaruddin. (2012). A comprehensive review of maximum power point tracking techniques for photovoltaic systems. *Renewable and Sustainable Energy Reviews, 16*(8), 5850-5862.

Jost, M., Pfreundt, A., & Witzmann, R. (2022). A review of bypass diodes in photovoltaic modules and systems. *Solar Energy, 237*, 233-247.

Kalogirou, S. A. (2009). *Solar energy engineering: Processes and systems*. Academic Press.

Karthick, R., Raj, R. S., & Kumar, S. S. (2019). A review of maximum power point tracking algorithms for photovoltaic systems under partial shading conditions. *Journal of Cleaner Production, 238*, 117865.

Kersten, W., Witte, T., & G. W. (2015). The influence of partial shading on the energy yield of PV systems. *Energy Procedia, 77*, 336-345.

King, D. L., Kratochvil, J. A., & Boyson, W. E. (1997). *Photovoltaic array performance model*. Sandia National Laboratories.

Kobayashi, K., Matsuo, H., & Sekine, Y. (2010). A novel topology of a partial-shading-tolerant PV module with distributed MPPT. *IEEE Transactions on Industrial Electronics, 57*(10), 3463-3470.

Kumar, N., & Sudhakar, K. (2020). A comprehensive review of the impact of dust on the performance of solar photovoltaic systems. *Renewable and Sustainable Energy Reviews, 134*, 110332.

Lopes, J. A. P., Madureira, A. G., & M. L. (2007). A new approach for modelling and simulation of PV modules with mismatch and shading effects. In *IEEE Power Tech, 2007* (pp. 1148-1153).

Malinowski, M., Stynski, S., & Goryca, Z. (2017). A review of MPPT techniques for photovoltaic systems under partial shading conditions. *Energies, 10*(11), 1845.

Marcos, J., Marroyo, L., Pulido, E., & Lorenzo, E. (2012). Mismatch losses in photovoltaic systems. *Renewable Energy, 41*, 290-295.

Marrou, L., Dandres, E., & Dufour, L. (2013). Impact of partial shading on the electrical performance of a PV module. *Energy Procedia, 40*, 362-369.

Mehedi, I. M., Salam, Z., & Ramli, M. Z. (2021). A review of global solar irradiance mapping and satellite-based estimation techniques. *Renewable and Sustainable Energy Reviews, 137*, 110599.

Müller, B. (2017). *Bypass diode thermal effects in photovoltaic modules*. Fraunhofer Verlag.

Nishioka, K., Sakitani, N., Uraoka, Y., & Fuyuki, T. (2007). Analysis of the shading effect on PV modules considering the bypass diode. *Solar Energy Materials and Solar Cells, 91*(19), 1716-1721.

Özkalay, E., Coşkun, M., & G. A. (2024). A review of maximum power point tracking algorithms for partially shaded photovoltaic systems. *International Journal of Hydrogen Energy, 52*(Part B), 1017-1033.

Parida, B., Iniyan, S., & Goic, R. (2011). A review of solar photovoltaic technologies. *Renewable and Sustainable Energy Reviews, 15*(3), 1625-1636.

Quaschning, V., & Hanitsch, R. (1996). Numerical simulation of current-voltage characteristics of photovoltaic arrays with shaded solar cells. *Solar Energy, 56*(6), 513-520.

Rani, B., Ilango, G. S., & Nagamani, C. (2013). A new single-stage fuzzy-based MPPT for PV systems under partial shading conditions. *IEEE Transactions on Industrial Electronics, 60*(11), 5007-5016.

Rezvani, A., Izadbakhsh, M., Gandomkar, M., & V. K. (2022). A review of optimisation strategies for maximum power extraction from photovoltaic systems under partial shading conditions. *Solar Energy, 238*, 141-163.

Sera, D., Teodorescu, R., & Rodriguez, P. (2006). PV panel model based on datasheet values. In *Proceedings of the IEEE International Symposium on Industrial Electronics, 2006* (Vol. 3, pp. 2392-2396).

SES Education. (n.d.). *SES TPS-3720 Solar Energy Trainer user manual*. Scientific Educational Systems.

Siddiqui, S. A., Adye, A., & Abusara, M. (2024). A novel MPPT technique for photovoltaic systems under partial shading conditions using Harris Hawks Optimisation. *Energies, 17*(1), 160.

Skoplaki, E., & Palyvos, J. A. (2009). On the temperature dependence of photovoltaic module electrical performance: A review of efficiency/power correlations. *Solar Energy, 83*(5), 614-624.

Subudhi, B., & Pradhan, R. (2013). A comparative study on maximum power point tracking techniques for photovoltaic power systems. *IEEE Transactions on Sustainable Energy, 4*(1), 89-98.

Tian, H., Wang, K., & Chen, Z. (2012). A novel MPPT algorithm for PV systems under partial shading conditions. *Energy Procedia, 16*, 1290-1296.

Tripathi, S., Mehrotra, A., & Gupta, A. (2019). A review on the modelling of photovoltaic arrays under partial shading conditions. *Journal of Renewable and Sustainable Energy, 11*(4), 042701.

Tsai, H. L., Tu, C. S., & Su, Y. J. (2008). Development of a generalised photovoltaic model using MATLAB/SIMULINK. In *Proceedings of the World Congress on Engineering and Computer Science 2008* (pp. 1-6).

Twidell, J., & Weir, A. D. (2015). *Renewable energy resources* (3rd ed.). Routledge.

Villalva, M. G., Gazoli, J. R., & Filho, E. R. (2009). Comprehensive approach to modelling and simulation of photovoltaic arrays. *IEEE Transactions on Power Electronics, 24*(5), 1198-1208.

Walker, G. R., & Sernia, P. C. (2004). Cascaded DC-DC converter connection of photovoltaic modules. *IEEE Transactions on Power Electronics, 19*(4), 1130-1139.

Wilson, G. M., Al-Jassim, M., & Metzger, W. K. (2020). The 2020 photovoltaic technologies roadmap. *Journal of Physics D: Applied Physics, 53*(49), 493001.

Woyte, A., Nijs, J., & Belmans, R. (2003). Partial shadowing of photovoltaic arrays with different system configurations: Literature review and field test results. *Solar Energy, 74*(3), 217-233.

Xuesong Zhou, X., & D. S. (2018). *Partial shading of photovoltaic systems: A review on analysis and mitigation techniques*. IET Renewable Power Generation.